UNIVERSITY OF SOUTHERN CALIFORNIA

DEPARTMENT OF CIVIL ENGINEERING

DEPENDENCE OF THE DURATION OF STRONG EARTHQUAKE GROUND MOTION ON MAGNITUDE, EPICENTRAL DISTANCE, GEOLOGIC CONDITIONS AT THE RECORDING STATION AND FREQUENCY OF MOTION

By

M. D. Trifunac and B. D. Westermo

Report No. CE 76-02

A Report on Research Conducted Under a Contract from the U.S. Nuclear Regulatory Commission

Los Angeles, California

November, 1976

ABSTRACT

A new definition of the duration of strong earthquake ground motion has been developed. It is based on the mean-square integral of motion (Trifunac and Brady, 1975) and employs the derivative of the smoothed integral of the time-function squared to compute the principal contribution to the duration of strong ground motion. This definition is directly related to the seismic energy recorded at a point and to the response spectrum amplitudes of linear viscously damped oscillator. Correlations have been presented which characterize duration of strong ground motion in terms of earthquake magnitude, epicentral distance, geologic environment of the recording stations and the frequency content of recorded motions.

INTRODUCTION

The duration of strong shaking is probably one of the least studied characteristics of strong earthquake ground motion (e.g., Bolt, 1973; Trifunac and Brady, 1975), yet it is one of the most important parameters for determining the destructive capabilities of an earthquake. Without some knowledge of the duration it is difficult to predict the non-linear and possibly deteriorating response of a structure. For the known duration of the motion as a function of frequency it is possible to determine the number of cycles through which a structure is stressed. The frequency dependent analysis of the duration of strong shaking is also useful in the studies of frequency dependent effects on attenuation and amplification of wave amplitudes.

We seek to characterize the duration of a certain frequency band of ground motion in terms of the parameters which describe the earthquake and the geological conditions at the recording station. We begin by defining the duration and by examining what implications that definition may have in the fields of earthquake engineering and strong-motion seismology. The definition of duration which we develop in this paper represents a refinement of the definition used by Trifunac and Brady (1975) and is based on the energy content of the recorded motion. We then examine the dependence of: (i) the integrals of acceleration, velocity and displacement squared, (ii) the duration and (iii) the average time rate of growth of integrals in (i), in six narrow frequency bands, on earthquake magnitude, epicentral distance, and recording site conditions.

The purpose of this paper is not to explore critically and in depth all the physical characteristics of the phenomena which characterize the duration of strong earthquake ground motion, but to present the currently available data on duration and the two related functionals of recorded strong motion accelerograms. Though we made every effort to characterize this data by simple regression equations and in terms of reasonable and approximate models which do not violate principles of wave propagation, the reader should recognize all stated and implied limitations of this analysis before attempting to apply our results and conclusions to a particular problem.

SOME DEFINITIONS

The integrals of the form $\int_0^T \begin{Bmatrix} a^2 \\ v^2 \\ d^2 \end{Bmatrix} dt$, where a(t), v(t) and d(t) represent the particle acceleration, velocity, and displacement and T is the total length of the record, are common in earthquake engineering. They appear (Arias, 1970; Housner, 1965) in the definitions of different measures of intensity, the expected values of the maxima of a(t), v(t), or d(t), and in the computations of seismic wave energy (Trifunac and Brady, 1975). These integrals also appear in the definition of the spectral widths, ϵ, of the power spectra of a(t), v(t), or d(t) which are given by (Cartwright and Longuet-Higgins, 1956)

$$\epsilon \begin{Bmatrix} a \\ v \\ d \end{Bmatrix} = 1 - \frac{m_2^2 \begin{Bmatrix} a \\ v \\ d \end{Bmatrix}}{m_0 \begin{Bmatrix} a \\ v \\ d \end{Bmatrix} m_4 \begin{Bmatrix} a \\ v \\ d \end{Bmatrix}} , \tag{1}$$

where the <u>nth</u> moment of a function computed from its energy spectrum $E(\omega)$ is

$$m_n = \int_0^\infty \omega^n E(\omega)\, d\omega . \tag{2}$$

Using Parseval's theorem, it is seen that the spectral width of the power spectrum of displacement, for example, is

$$\epsilon(d) = 1 - \frac{\left(\int_0^\infty v^2 dt\right)^2}{\int_0^\infty a^2 dt \int_0^\infty d^2 dt} . \qquad (3)$$

The nature of the growth of the integrals

$$\int_0^t \begin{Bmatrix} a^2 \\ v^2 \\ d^2 \end{Bmatrix} d\tau , \qquad \text{for } 0 \le t \le T ,$$

versus time t and for typical acceleration, velocity and displacement records is shown in Figure 1. In most cases, these integrals increase rapidly and then tend asymptotically towards their final values $\int_0^T a^2 dt$, $\int_0^T v^2 dt$, and $\int_0^T d^2 dt$, where T is the total duration of a(t), v(t) or d(t) records. The motions recorded during the time interval over which these integrals slowly tend to their final values correspond to the later arrivals of scattered waves attenuated along their longer paths. The rapid growth of these integrals results from the arrival of the strongest contributions to the functions a(t), v(t), or d(t). However, if we look at such integrals for different frequency bands of the original function, their general shape will differ from one frequency band to the other due to the different arrival times caused by the reflections and scattering for waves of different frequencies. It is the time intervals during which the largest contributions to these integrals take place in a given frequency band that we consider to represent the duration of "strong ground motion" in that frequency band.

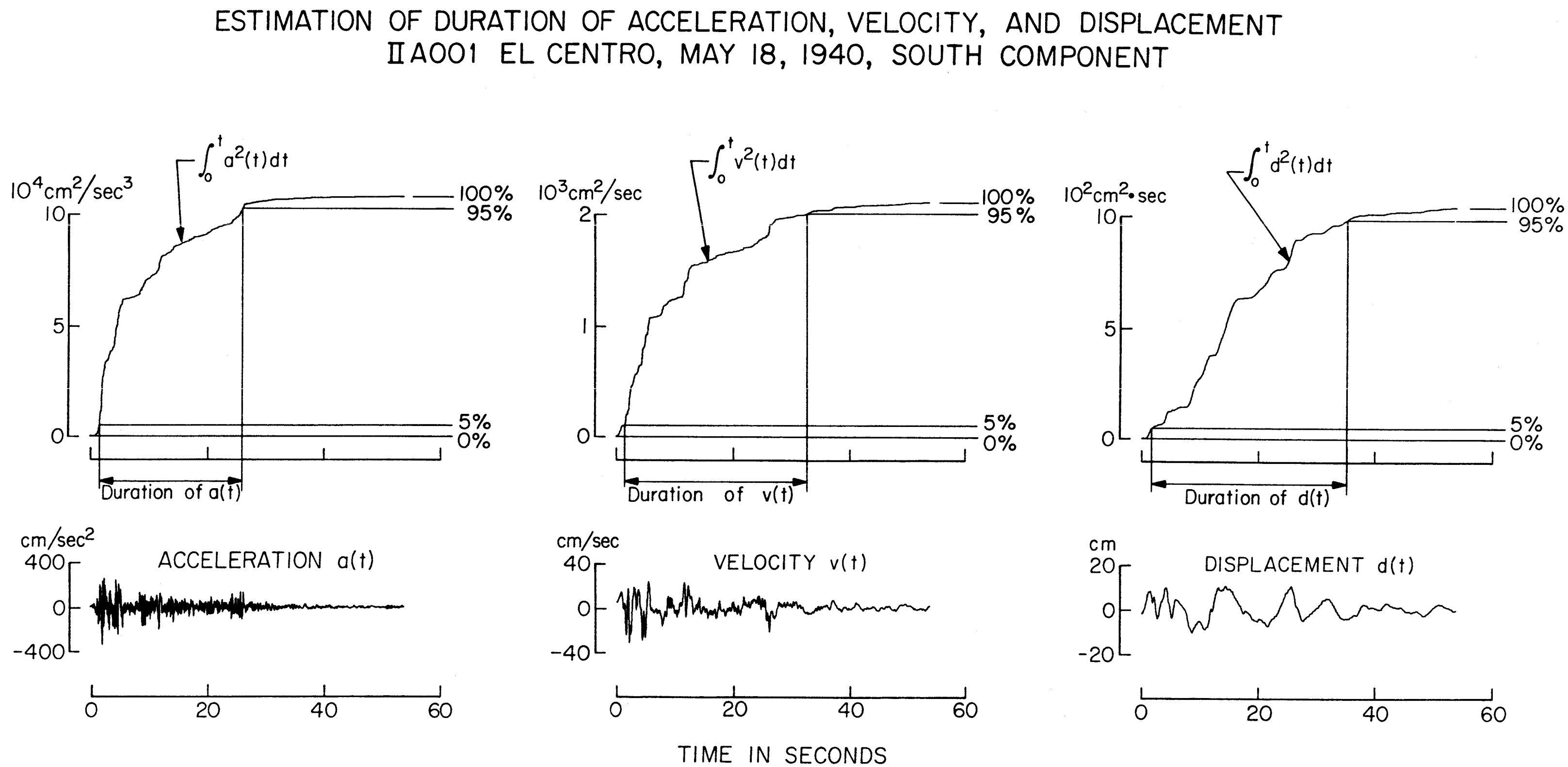

Figure 1. Definition of the durations of acceleration, velocity and displacement (from Trifunac and Brady, 1975)

In seeking a useful definition which would specify the time intervals contributing most to these integrals, we seek a method which is least related to other parameters which characterize the motion (particularly one independent of amplitude) and is based on the shape of $\int_0^t f^2 d\tau$ versus t. In a previous study of the duration of strong ground motion (Trifunac and Brady, 1975), the first 5% and the last 5% of the amplitudes of these integrals were deleted and the "middle" 90% of the total amplitude of $\int_0^T f^2 d\tau$ was considered to be representative of the strong ground motion. The duration was taken as the time during which this contribution took place.

On examining some of these integrals in detail (Figure 1), we find that some of them may not tend to their final value, $\int_0^T f^2 d\tau$, as uniformly as others, and thus by simply deleting the upper 5% it is possible that the ending time of the "strong motion" may be too large. Another possible difficulty that might result from applying this simplified definition to the present work is that we are considering frequency band-filtered data of a(t), v(t), and d(t), and because of the different characteristics of seismic waves within different frequency bands this definition may not apply uniformly to all the frequency bands. Furthermore, the above simple definition may not be adequate for structural response analyses when several separate time intervals, over which the significant contributions to the total integrals are made, are present. Finally, if one were to assume that the exponential frequency dependent attenuation of the form, $e^{-\frac{\Delta\omega}{2Q\beta}}$, is representative for the data at hand, the high frequency waves could be attenuated more rapidly, and thus reflected waves that have travelled longer paths could contribute less to the integrals. On the other hand, low frequency waves might not be as strongly attenuated, and thus reflected and scattered late arrivals could contribute more to the total value of the integrals at later times.

If one were to record a strong pulse of energy arriving at a station which is followed by another pulse arriving at some later time, the definition used by Trifunac and Brady (1975) could yield a duration that corresponds approximately to the length of time between the two pulses. However, the actual motion could be quite small during the time interval between the two pulses. Therefore, to avoid these and other similar difficulties, in this paper we define the total duration of a frequency-band-limited record f(t) [f(t) represents a(t), v(t) and/or d(t)] to be the sum of the time intervals during which the largest contribution to the total value of $\int_0^T f^2 d\tau$ is made. We require these largest contributions to be made during the time intervals for which the slopes of the integral curves are the largest. Thus, if one calculates the derivatives of the smoothed integrals, $\int_0^t f^2(\tau)d\tau$, it is possible to define the total duration to be the sum of the time intervals during which this derivative is greater than some value. We choose that value so that the area under the smoothed derivative during these time intervals corresponds to some given percentage of the total area,

$\int_0^T f^2 d\tau$ (see Figure 2). Since, in general, the integrals, $\int_0^t f^2 d\tau$, are not smooth functions, their derivatives will not be smooth and will consist of many sharp peaks of short duration. However, one can smooth the function $\int_0^t f^2(\tau)d\tau$ before differentiating to avoid having too many intervals contributing to the strong motion duration and yet without significantly altering the total length of the time intervals involved. Such a smoothed $\int_0^t f^2(\tau)d\tau$ curve and its derivative are shown in Figure 2. As it can be seen from this figure, this definition yields several contributing intervals which are separated by weaker arrivals. The total sum of these time intervals represents the duration for this particular record. The use of this definition in the previous study by Trifunac and Brady (1975) would tend to reduce the scatter of the computed durations.

For simplicity, but quite arbitrarily, we have used 90% of the total amplitudes of the integrals to compute the duration of strong-motion in this paper. Figure 3 shows the histograms of the ratios of the durations computed for a 90% limit to the durations based on 70% and 80% limits for all records used in this analysis. From these and other similar distributions, the durations for any other desired percentage limit that may best fit some particular applications could be inferred from the correlations based on a 90% limit.

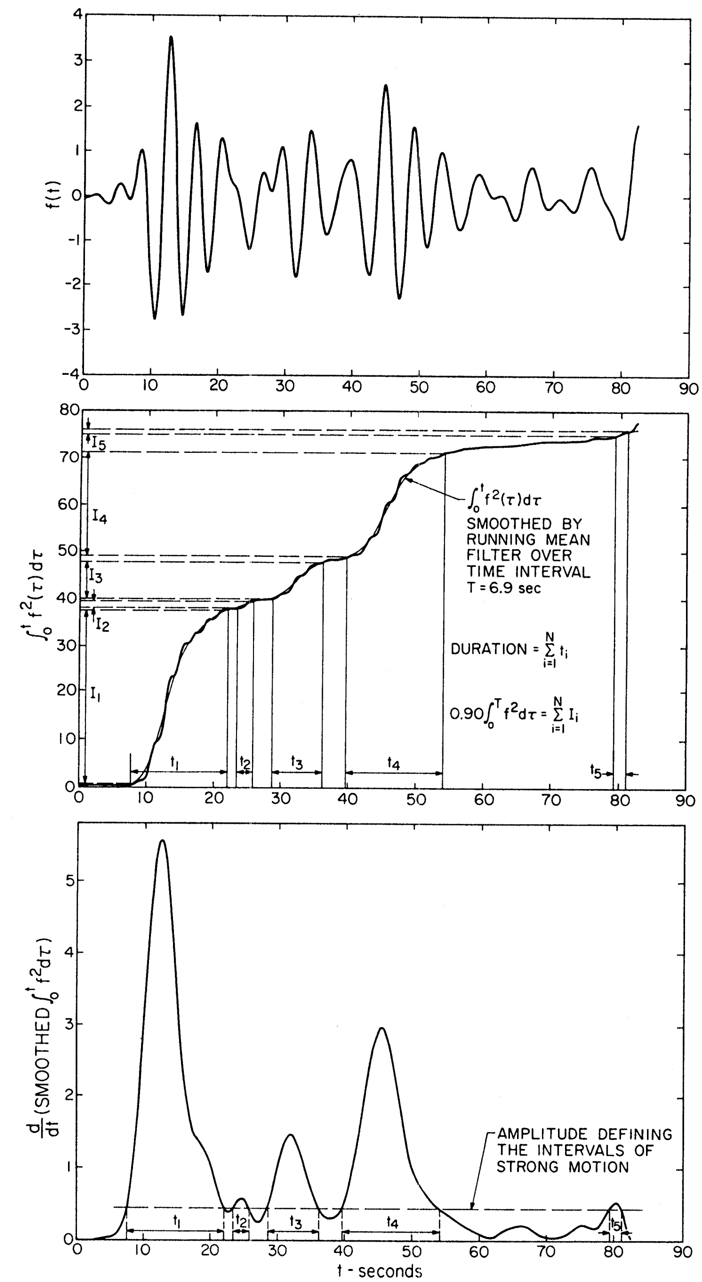

Figure 2. Top: Record for displacement from Kern County earthquake after application of the band-pass filter centered at 0.22 cps. Middle: Comparison of $\int_0^t f^2(\tau)d\tau$ computed for f(t) in the top figure with its smoothed form. Bottom: The derivative of the smoothed function, $\int_0^t f^2(\tau)d\tau$, showing the intervals of strong motion as defined in this paper.

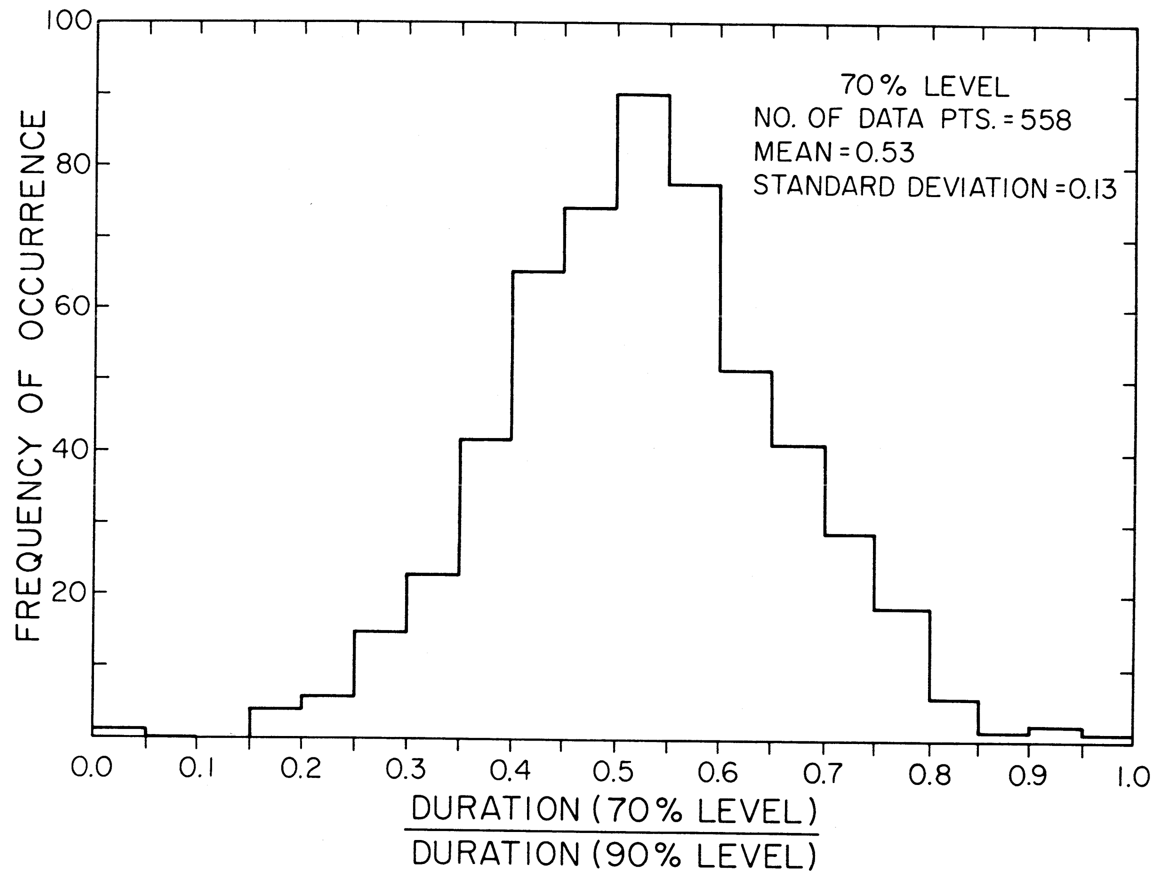

Figure 3a. Frequency of occurrence of the ratios of duration for a 70 percent limit of $\int_0^T f^2 dt$ with the duration for a 90 percent limit.

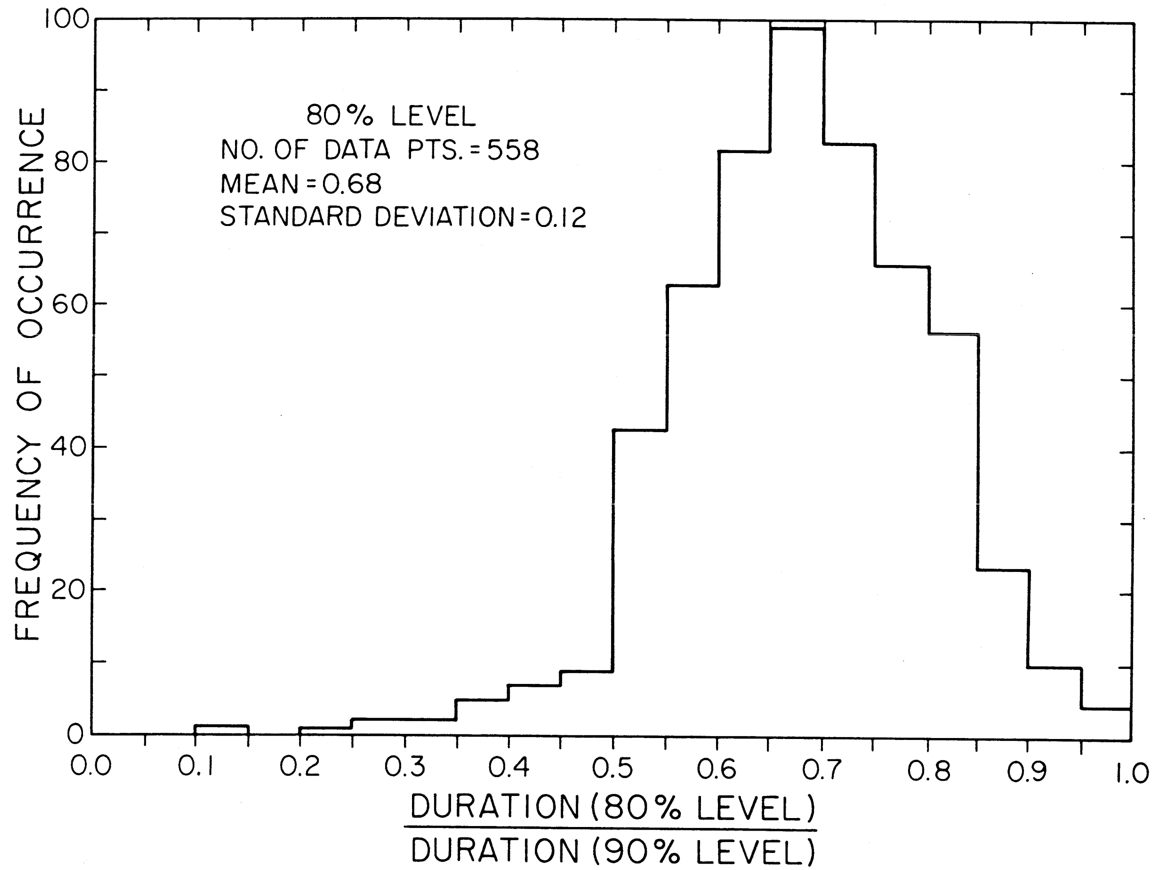

Figure 3b. Frequency of occurrence of the ratios of duration for a 80 percent limit of $\int_0^T f^2 dt$ with the duration for a 90 percent limit.

The slope of the integral $\int_0^t f^2(\tau)\,d\tau$, or power,* represents another useful quantity in the analysis of strong ground motion in that it corresponds or is analogous to the rate at which seismic energy within a frequency band passes a station. We see from the above definition that the duration as we define it in this paper corresponds to the time interval during which the largest time average of power is recorded at a station.

Whether a structure is modeled by a linear, viscously damped system or by a nonlinear, hysteretic system, it is evident that it can absorb only a finite amount of energy per unit time before it begins to weaken its components to accommodate the excess power input. For example, a structure might develop cracks or plastic hinges to allow for the increase in energy dissipation necessary. Although the total amount of energy fed into a structure may be quite large (i.e., $\int_0^T f^2 d\tau$ being large), if the time interval during which this occurs is very long relative to the fundamental period of the system, i.e., the input power is low, the structure may be able to absorb most of the input energy and may remain undamaged. Conversely, if the power input is large and persists for an extended period of time, serious damage to the structure may result to accommodate the high rate of energy input.

---

*In this paper we will often refer to the time rate of growth of integrals of the form $\int_0^t f^2(\tau)\,d\tau$ as "power," only to emphasize the general analogy implied by the form of these integrals which can be associated with total "energy" contained in f(t) for $0 \le t \le T$.

In this analysis we define the average power as

$$\text{RATE} \equiv \int_0^T f^2 dt/\text{duration of strong motion} \qquad (4)$$

This rate is proportional to $\overline{f^2}$, the mean-square value of f(t) evaluated over the duration, i.e., $\overline{f^2} \doteq 0.9 \cdot$ Rate since we select T to correspond to $0.9 \int_0^T f^2 dt$.

DESCRIPTION OF DATA AND AN OUTLINE OF CALCULATIONS

The acceleration, velocity, and displacement data used in this study are taken from the Volume II tapes (Trifunac and Lee, 1973) which contain corrected accelerograms and integrated velocity and displacement curves. These data result from the strong ground motion recording program in the Western United States and have been processed for the period beginning in 1933 and ending in 1971. The data consists of 186 accelerograph records (372 horizontal and 186 vertical components) which were obtained at "free-field" stations or in the basement floors of buildings. These data are a result of 49 earthquakes whose magnitudes range from 3.0 to 7.7. Of the 186 records, 5 or 3% correspond to the magnitude range 4.0-4.9, 40 or 22% to 5.0-5.9, 126 or 69% to 6.0-6.9, and 7 or 4% to the magnitude range 7.0-7.9. Six of the 186 records were not used in this analysis because of incomplete information on magnitude. Sixty-five percent of these 180 records have been recorded on alluvium sites, 28% on "intermediate" sites, and 7% on basement rock sites. All the accelerograph stations that recorded on alluvium or otherwise "soft" sedimentary deposits have been classified under $s = 0$. The sites located on hard basement rocks were labeled by $s = 2$, whereas the sites located on "intermediate" type rocks or in a complex environment which could not be identified as either $s = 0$ or $s = 2$ have all been grouped under $s = 1$ (Trifunac and Brady, 1975).

The complete records from the Volume II tapes (Trifunac and Lee, 1973) were filtered with an Ormsby digital low-pass filter in succession by filtering each low-pass filtered record with a progressively lower roll-off and termination frequency. Six narrow frequency bands were generated in this manner for this analysis. The sum of all these six band-pass filtered records adds up to the complete original record. The original data on the Volume II tapes is in the 0.125 to 25 cycles per second frequency range where 0.125 cps corresponds to the 8 sec filters used for all of the 70- and 35-mm film records which have been presented in the Volume II series. Other accelerograms which were recorded on paper records have been high-pass filtered from 0.07 cps. For simplicity in this work and because many records in the Volume II data set are available for frequencies greater than 0.125 cps only, we will not consider frequencies lower than 0.125 cps.

The transfer functions for the six filters are shown in Figure 4. Table I lists the roll-off and termination frequency of each of the six low-pass filters used. The integrals, $\int_0^t f^2(\tau)d\tau$, for the six frequency bands of acceleration, velocity, and displacement records were then calculated and these functions were smoothed by a running mean filter with the time windows given in Table I. These smoothed functions were next numerically differentiated to produce functions similar to that shown in Figure 2c. A cut-off amplitude for this differentiated function as shown in Figure 2c is chosen so that the sum of the areas under the differentiated curve during the time intervals when this function exceeds this limit is equal to 0.9 of the final value of the integral $\int_0^T f^2 d\tau$.

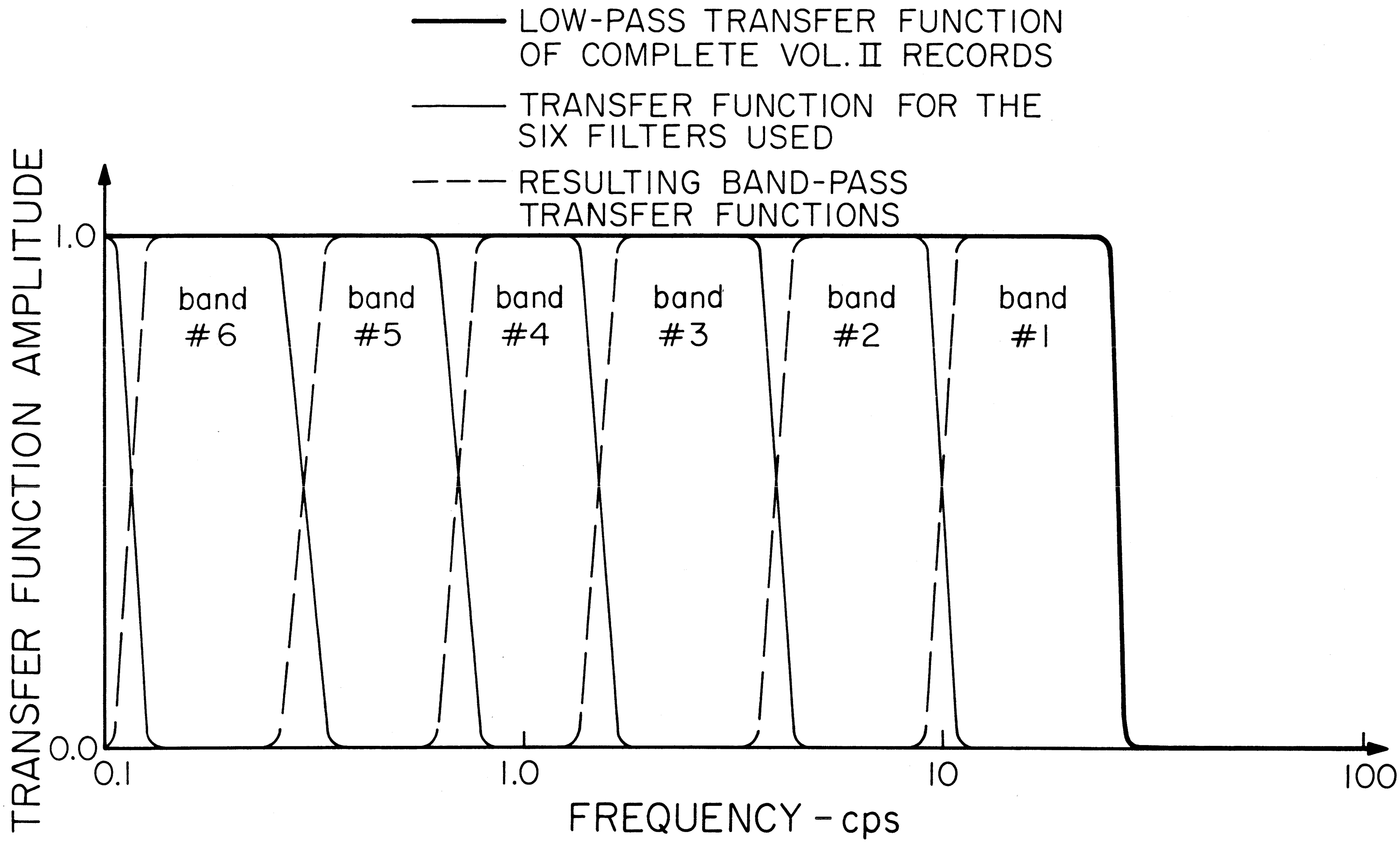

Figure 4. Transfer functions of the six band-filters used in this paper.

TABLE I

Roll-Off and Termination Frequencies for the Six Low-Pass Ormsby Filters (Figure 4) and Filter Windows for Smoothing the Integrals $\int_0^t f^2(\tau)d\tau$

Band No.	Low-Pass Roll-Off Frequency (cps)	Low-Pass Termination Frequency (cps)	Center Frequency (cps)	Filter Window* (sec)
1	9.1	10.9	18.0	3.38
2	3.6	4.4	7.0	3.38
3	1.34	1.66	2.7	3.38
4	0.62	0.78	1.1	4.08
5	0.26	0.34	0.5	4.08
6	0.105	0.125	0.2	6.9

*Filter window represents the time interval in seconds over which the running mean filter was used to low-pass filter $\int_0^t f^2(\tau)d\tau$ (see also Figure 2b).

CORRELATIONS OF $\int_0^T a^2 dt$, $\int_0^T v^2 dt$, AND $\int_0^T d^2 dt$ WITH EPICENTRAL DISTANCE, MAGNITUDE, AND SITE CLASSIFICATION

The correlations of $\int_0^T a^2 dt$, $\int_0^T v^2 dt$, and $\int_0^T d^2 dt$ for six narrow frequency bands with earthquake magnitude, M, epicentral distance, Δ, and site classification, s (s = 0 for alluvium, s = 1 for intermediate rocks, and s = 2 for igneous basement rocks), are presented in this section. Because of our incomplete knowledge of what the actual functional relationships are that govern these correlations, and because the number of recorded data is quite limited, we consider only an approximate simple regression equation,

$$\log_{10}\left\{\int_0^T \begin{pmatrix} a^2 \\ v^2 \\ d^2 \end{pmatrix} dt\right\} = as + bM + c\Delta + d + e\log_{10}A_0(\Delta) + fM^2 , \quad (5)$$

in which we select the number and the order of terms to satisfy only the essential principles of wave propagation. a, b, . . . , e & f on the right hand side of equation (5) are as yet unknown "coefficients" which will be determined from the regression analysis of $\log_{10}\left\{\int_0^T \begin{pmatrix} a^2 \\ v^2 \\ d^2 \end{pmatrix} dt\right\}$ computed from recorded accelerograms.

We have selected a, b, c, d, e and f to represent frequency dependent coefficients in this and subsequent regression analyses in this paper, and to save effort in writing we have often omitted explicit indication that they depend on $\omega_c = 2\pi f_c$, i.e. $a(\omega_c), b(\omega_c), \ldots, f(\omega_c)$. At the same time on the left hand side of all regression equations we have chosen to identify time dependent acceleration, velocity and displacement with a, v and d, respectively. Although this leads to twofold meaning of symbols "a" and "d" the reader should not have any difficulty in precisely interpreting our equations since a, v, and d representing a(t), v(t) and d(t) are always separated from "coefficients" a, b, . . . , f.

The site conditions of an accelerograph station can affect the recorded motions in a complicated way. However, the rough classification of such site conditions into three groups (Trifunac and Brady, 1975) and the uneven distribution of the data among these groups ($s = 0$, 1 and 2) suggest the use of only the simplest linear form for this dependence as the term as in equation (5). When a greater number of accelerograms becomes available and with better and more detailed site classifications, it will become possible to add higher order terms to the site classification term and to include its dependence on amplitudes of wave motions and the type of waves involved. The term $\log_{10} A_0(\Delta)$ (Table II) represents a smoothed version of the empirically determined function (Richter, 1958) which describes the attenuation of wave amplitudes with epicentral distance, Δ, in California. Since most of the strong-motion data which are analyzed in this paper are also from California, this function represents a fair approximation for amplitude attenuation with distance (Trifunac, 1976b).

The terms $bM + fM^2 + d$ in equation (5) represent the approximate scaling of the integrals with respect to magnitude, which is for most recordings represented by the local magnitude, M_L (Richter, 1958). This functional form has been motivated by several related studies (e.g., Trifunac, 1976a, 1976b) and by the empirical relation (Gutenberg and Richter, 1956) $\log E = 9.4 + 2.14M_L - 0.054M_L^2$, where E is the energy radiated in elastic waves in ergs. Here, as in the correlation with

TABLE II

$\log_{10} A_0(\Delta)$ Versus Epicentral Distance Δ

(only the first two digits may be assumed to be significant)

Δ (km)	$-\log_{10} A_0(\Delta)$	Δ (km)	$-\log_{10} A_0(\Delta)$	Δ (km)	$-\log_{10} A_0(\Delta)$
0	1.400	140	3.230	370	4.336
5	1.500	150	3.279	380	4.376
10	1.605	160	3.328	390	4.414
15	1.716	170	3.378	400	4.451
20	1.833	180	3.429	410	4.485
25	1.955	190	3.480	420	4.518
30	2.078	200	3.530	430	4.549
35	2.199	210	3.581	440	4.579
40	2.314	220	3.631	450	4.607
45	2.421	230	3.680	460	4.634
50	2.517	240	3.729	470	4.660
55	2.603	250	3.779	480	4.685
60	2.679	260	3.827	490	4.709
65	2.746	270	3.877	500	4.732
70	2.805	280	3.926	510	4.755
80	2.920	290	3.975	520	4.776
85	2.958	300	4.024	530	4.797
90	2.989	310	4.072	540	4.817
95	3.020	320	4.119	550	4.835
100	3.044	330	4.164	560	4.853
110	3.089	340	4.209	570	4.869
120	3.135	350	4.253	580	4.885
130	3.182	360	4.295	590	4.900

the site conditions, we do not use more detailed functional dependence on M because the distribution of the available data among different magnitude intervals is not uniform (59% of the data being for the magnitude range 6.0 to 6.9 alone).

It is seen from $bM + fM^2 + d$ that this term reaches its maximum for $M_{max} = -b/2f$ and that its amplitudes then decrease for $M \geq M_{max}$. Since such behavior is not acceptable on a physical basis, we employ this function for $M \leq M_{max}$ only and for $M \geq M_{max}$ assume the form $bM_{max} + fM_{max}^2 + d$. This choice of magnitude dependence of integrals in (5) is, of course, quite arbitrary and will have to be reviewed and improved when more data becomes available for magnitudes greater than 7.

The function $\log_{10} A_0(\Delta)$ is a frequency independent term which models the overall amplitude attenuation for a broad frequency band of seismic waves. However, when considering the narrow frequency bands as in this study, the degree of attenuation of the amplitudes with distance may change with the different narrow frequency bands, since the predominant type of wave motion may be different within each band. Thus, the coefficient e would be expected to change with frequency depending on the relative contribution to attenuation from the other term $c\Delta$. This other distance dependent term in (5), $c\Delta$, has been chosen to represent the frequency dependent exponential attenuation of the form

$$f(\omega, \Delta) = e^{-\frac{\omega \Delta}{2Q\beta}} \qquad (6)$$

where $f(\omega, \Delta)$ is the attenuation factor, β is the wave velocity, is the wave frequency, Δ represents distance, and Q is a factor characterizing the medium.

Table III presents the least-squares fitted coefficients in the correlation (5) for the horizontal and vertical components of acceleration, velocity, and displacement records and for each of the six narrow frequency bands. If we assume that each of the frequency bands is sufficiently narrow with the data being essentially at the center frequency of each band, $\omega_c = 2\pi f_c$, we can average the data in Table III for acceleration, velocity, and displacement. Thus, assuming that the displacement data for each frequency band are essentially at the frequency ω_c, one can write

$$|v(t)| \doteq |\omega_c d(t)|$$

$$|a(t)| \doteq |\omega_c^2 d(t)| \, , \qquad (7)$$

and thus

$$\log_{10} \int_0^T d^2 dt \doteq \log_{10} \int_0^T a^2 dt - 4 \log_{10} \omega_c$$

$$\log_{10} \int_0^T v^2 dt \doteq \log_{10} \int_0^T a^2 dt - 2 \log_{10} \omega_c \, . \qquad (8)$$

Therefore, the estimates of a, b, c, e, and f versus frequency should not vary much from acceleration to velocity and to displacement. The coefficient d should be expected to vary by $2 \log_{10} \omega_c$ and $4 \log_{10} \omega_c$ from acceleration to velocity and acceleration to displacement, respectively.

Assuming that equations (8) are valid, the corresponding coefficients were averaged. Because of the small signal-to-noise ratio for data like the high frequency displacements (band no. 1, $f_c = 18$ cps) and

TABLE III

Regression Coefficients in

$$\log_{10} \int_0^T \begin{Bmatrix} a^2 \\ v^2 \\ d^2 \end{Bmatrix} dt = as + bM + c\Delta + d + e \log_{10} A_0(\Delta) + fM^2 \pm \sigma$$

$$M \leq M_{max}$$

$$\sigma = A + B \log_{10} \Delta \pm \Sigma$$

Vertical Motion

ACCELERATION

f_c =	18.0	7.0	2.7	1.1	0.5	0.2
a	.041	-.073	-.207	-.112	-.288	-.262
b	7.54	5.88	5.15	4.28	5.56	4.55
c	-.009	-.008	-.0016	-.004	-.001	-.007
d	-21.9	-16.4	-14.3	-11.0	-16.2	-15.0
e	.998	.639	.873	.695	.864	.004
f	-.526	-.401	-.339	-.282	-.364	-.292
σ	.648	.495	.455	.423	.584	.606
A	.719	.618	.776	.660	1.04	.801
B	-.136	-.144	-.247	-.200	-.354	.190
Σ	.417	.314	.255	.259	.345	.355
M_{max}	7.17	7.33	7.60	7.59	7.63	7.79

VELOCITY

a	.036	-.084	-.224	-.130	-.289	-.219
b	7.19	5.58	5.14	4.03	5.45	4.45
c	-.009	-.008	-.0014	-.004	-.002	-.007
d	-24.9	-18.6	-15.9	-12.7	-17.1	-14.7
e	.932	.601	.906	.662	.757	-.029
f	-.499	-.379	-.335	-.262	-.355	-.294
σ	.630	.484	.459	.422	.595	.567
A	.687	.649	.743	.678	1.006	.638
B	-.126	-.169	-.225	-.208	-.323	-.110
Σ	.407	.307	.260	.250	.347	.335
M_{max}	7.20	7.36	7.67	7.69	7.68	7.57

DISPLACEMENT

a	-.009	-.092	-.216	-.124	-.267	-.233
b	7.23	5.36	4.80	3.68	4.99	3.98
c	-.005	-.008	-.002	-.004	-.003	-.007
d	-28.3	-21.0	-16.6	-13.9	-16.6	-13.5
e	1.07	.585	.800	.644	.579	-.119
f	-.506	-.362	-.309	-.235	-.322	-.259
σ	.536	.477	.446	.417	.605	.529

TABLE III (Continued)

(Vertical Motion Continued)

DISPLACEMENT (Continued)

f_c =	18.0	7.0	2.7	1.1	0.5	0.2
A	.834	.670	.749	.633	.949	.684
B	-.265	-.184	-.231	-.182	-.284	-.166
Σ	.350	.300	.244	.246	.357	.333
M_{max}	7.14	7.40	7.77	7.82	7.75	7.68

Horizontal Motion

ACCELERATION

f_c	18.0	7.0	2.7	1.1	0.5	0.2
a	.098	-.050	-.272	-.129	-.407	-.451
b	8.64	7.19	4.86	4.82	5.95	5.72
c	-.001	-.010	-.0015	-.006	.001	-.008
d	-25.3	-20.1	-12.6	-12.0	-16.7	-17.9
e	.792	.512	.899	.662	1.06	.137
f	-.626	-.512	-.317	-.326	-.391	-.381
σ	.641	.511	.530	.444	.595	.703
A	.783	.466	.775	.620	.800	1.002
B	-.181	-.046	-.221	-.172	-.214	-.264
Σ	.417	.330	.328	.287	.387	.409
M_{max}	6.90	7.02	7.67	7.39	7.61	7.50

VELOCITY

a	.093	-.016	-.302	-.171	-.423	-.410
b	8.52	7.26	5.30	5.09	6.31	5.59
c	-.001	-.009	-.001	-.005	-.0004	-.008
d	-29.0	-23.3	-15.5	-15.1	-19.1	-18.0
e	.744	.558	.965	.698	.913	.038
f	-.617	-.519	-.351	-.348	-.417	-.370
σ	.639	.508	.554	.451	.600	.709
A	.814	.488	.849	.639	.770	.936
B	-.202	-.058	-.254	-.179	-.189	-.218
Σ	.417	.324	.341	.288	.384	.408
M_{max}	6.90	6.99	7.55	7.31	7.56	7.56

TABLE III (Concluded)

(Horizontal Motion Continued)

DISPLACEMENT

f_c	18.0	7.0	2.7	1.1	0.5	0.2
a	-.024	-.033	-.287	-.200	-.427	-.424
b	7.38	7.33	5.05	4.87	5.81	5.76
c	-.004	-.009	-.001	-.004	-.0007	-.009
d	-28.9	-26.4	-16.4	-16.6	-18.4	-18.4
e	.883	.602	.938	.719	.900	-.046
f	-.521	-.524	-.330	-.331	-.378	-.394
σ	.498	.509	.548	.458	.610	.672
A	.791	.527	.820	.672	.859	.851
B	-.262	-.080	-.237	-.194	-.234	-.185
Σ	.336	.323	.333	.288	.377	.391
M_{max}	7.08	6.99	7.65	7.36	7.68	7.31

low frequency accelerations (band no. 6, $f_c = 0.2$ cps), these data were not used in computing the coefficients in Figure 5. The range between the mean plus and the mean minus the largest of the differences between the mean and each of the actual values is presented for all the coefficients in Figure 5. This figure shows the coefficients for acceleration, and equation (8) gives the necessary relations to calculate

$\log_{10} \int_0^T v^2 dt$ and $\log_{10} \int_0^T d^2 dt$.

For the dependence on the site conditions the range of values of $\int_0^T \begin{Bmatrix} a^2 \\ v^2 \\ d^2 \end{Bmatrix} dt$ is larger at low frequencies than at higher frequencies as shown by Figure 5. For the low frequency band $f_c = 0.2$ cps, empirical scaling in terms of equation (5) indicates that the amplitudes of those integrals are about seven times smaller for horizontal motion and three times smaller for vertical motion at a "hard" site ($s = 2$) than at a "soft" site ($s = 0$). At the high frequency end ($f_c = 18.0$ cps) the amplitudes of $\int_0^T \begin{Bmatrix} a^2 \\ v^2 \\ d^2 \end{Bmatrix} dt$ at hard ($s = 2$) sites are up to 1.5 times larger than those for soft ($s = 0$) sites. The greater difference between the values of the coefficient a in equation (5) for the vertical and horizontal motion at the lower frequencies is most likely caused by the different nature of motion for the various low frequency waves having vertical or horizontal predominance of motion. At higher frequencies this difference decreases probably because of the greater degree of "mixing" of short period waves which are more sensitive to various inhomogeneities along their propagation paths.

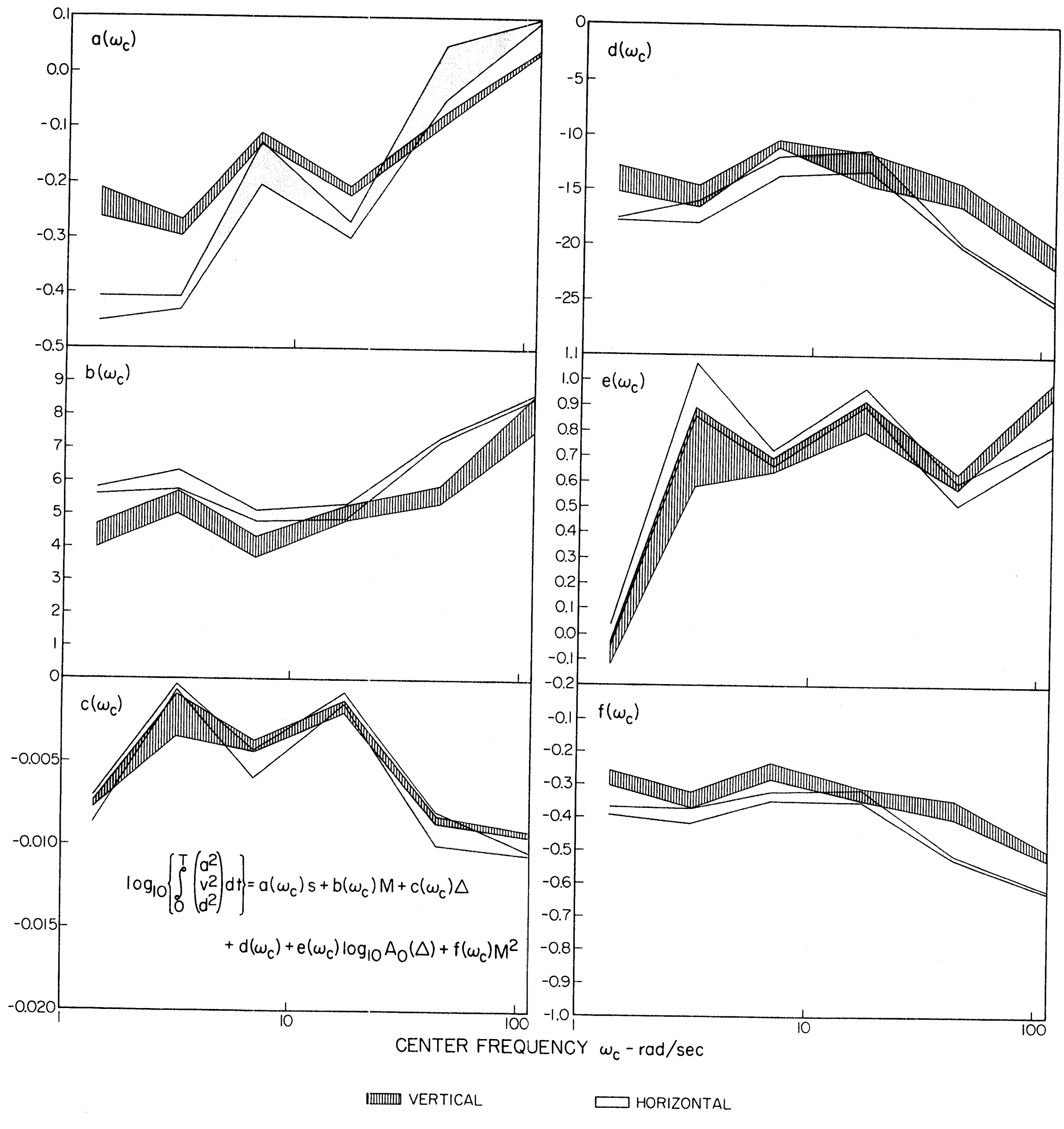

Figure 5. Coefficients a, b, c, d, e and f in equation (5) for horizontal and vertical components of acceleration, plotted versus $\omega_c = 2\pi f_c$ (for f_c = 0.2, 0.5, 1.1, 2.7, 7.0 and 18.0). Corresponding results for velocity and displacement can be obtained from equations (8).

Assuming that each of the frequency bands is narrow so that the data within each band can be described by its center frequency, $\omega_c = 2\pi f_c$, we find that the physical meaning of the coefficient c would be

$$c \doteq -\frac{0.21}{Q^*\beta}\omega_c \qquad (9)$$

where Q^* is the average value of Q for the corresponding frequency band.

If the empirical function $\log_{10} A_0(\Delta)$ were to describe the geometric attenuation effects within a narrow frequency band only, the term $c\Delta$ in equation (5) could be thought of as an approximate model for anelastic and other forms of attenuation excluding the geometric spreading. Then, it could be expected that Q^* in (9) represents an average value of the Q's for the data in that frequency band. But, since $\log_{10} A_0(\Delta)$ represents the empirically derived attenuation law, it models approximately the overall average amplitude changes with distance and thus includes both geometric and anelastic attenuation effects. The parameter c can therefore be thought of as containing a correction term for $e \log_{10} A_0(\Delta)$ to include the frequency dependent anelastic attenuation as follows

$$c\Delta + e \log_{10} A_0(\Delta) = c\Delta + e\{f(\Delta) + \eta\Delta\} . \qquad (10)$$

Ideally, $f(\Delta)$ would represent a function which describes geometric attenuation for the seismic waves within a given frequency band, and η a frequency dependent constant so that c^* in

$$c^* = c + e\eta \qquad (11)$$

reflects the average value of Q for the corresponding frequency band as in (9).

The estimates of e for the five highest center frequencies (Figure 5) are nearly constant, but they drop off at the lowest frequency band ($f_c = 0.2$). This probably results from the small signal to noise ratio for low frequency bands where the digitization noise, which does not decrease with Δ, may tend to diminish the role of $\log_{10} A_0(\Delta)$ term in equation (5).

By comparing the values of $bM + fM^2 + d$ for different frequency bands, we see that $\log_{10} \int_0^T \begin{Bmatrix} a^2 \\ v^2 \\ d^2 \end{Bmatrix} dt$ changes by several orders of magnitude from one frequency band to the next for a given magnitude. The value of $\int_0^T \begin{Bmatrix} a^2 \\ v^2 \\ d^2 \end{Bmatrix} dt$ for magnitude of 7.0 is about 10^5 times the value of $\int_0^T \begin{Bmatrix} a^2 \\ v^2 \\ d^2 \end{Bmatrix} dt$ for a magnitude of 4.0.

The maxima of the curves $bM + fM^2$ for both horizontal and vertical components and for all frequency bands are consistently between M = 7.0 and M = 8.0 and typically $M_{max} \doteq 7.6$ (Figure 6). Therefore, for values of M larger than M_{max} we use

$$\log_{10} \int_0^T \begin{Bmatrix} a^2 \\ v^2 \\ d^2 \end{Bmatrix} dt = as + c\Delta + bM_{max} + fM_{max}^2 + d \; . \qquad (12)$$

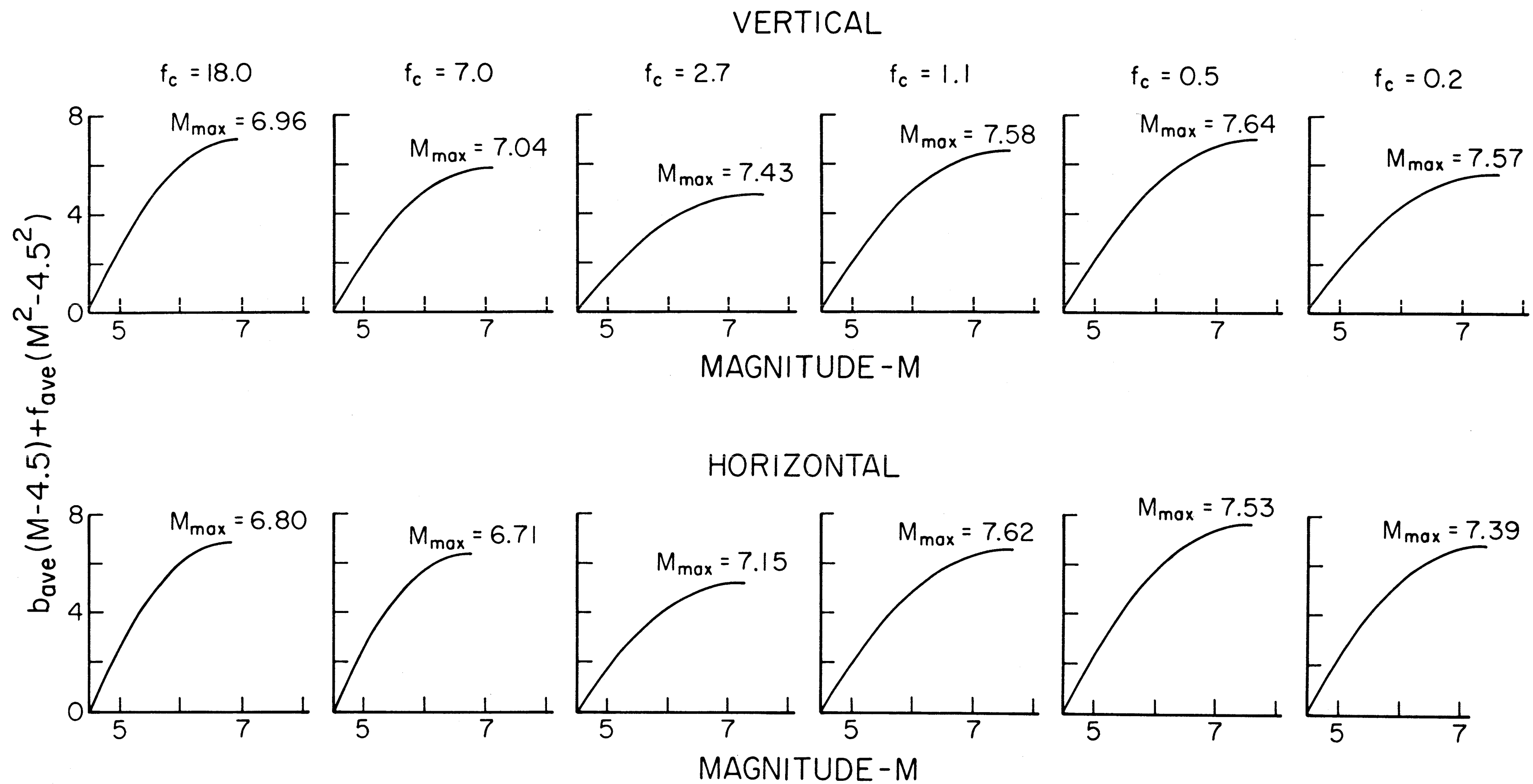

Figure 6. Contribution to $\log_{10} \int_0^T \begin{Bmatrix} a^2 \\ v^2 \\ d^2 \end{Bmatrix} dt$ in equation (5) from the average values of $bM + fM^2$.

These results are in agreement with other related studies of localized strong motion effects (Trifunac, 1976a, 1976b) which also suggest that the overall amplitudes of the near-field strong earthquake ground motion may cease to grow for magnitudes greater than about M = 7.5. This can be explained by the fact that large magnitudes when computed from the amplitudes of long period teleseismic waves usually imply large fault dimensions (hundreds of km), while strong-motion amplitudes (for frequencies between 0.125 cps and 25 cps) studied in this paper appear to be primarily influenced by the local (tens of km) details of faulting. Figure 6 presents the amplitudes of $b_{ave}M + f_{ave}M^2$ for the average values of b and f shown in Figure 5 for six frequency bands and for the horizontal and vertical components of motion. For ease in presentation these curves are all normalized with respect to M = 4.5.

To examine the dependence of the standard deviation of the data points with respect to the regression equation (5) on distance, the following regression was used

$$\sigma = A + B \log_{10} \Delta \pm \Sigma . \qquad (13)$$

The coefficients A, B and the standard deviation Σ are given in Table III. Examination of these data shows that σ decreases with increasing distance, Δ. This decrease is nearly constant for all frequency bands.

Figures 7a and 7b present a summary of the overall dependence of $\log_{10} \int_0^{T'} a^2 dt$ on magnitude, M, site classification, s, distance, Δ, and component direction. For each epicentral distance in this figure we present a range of values for these integrals to show the uncertainty associated with the use of equation (5). The range of values for

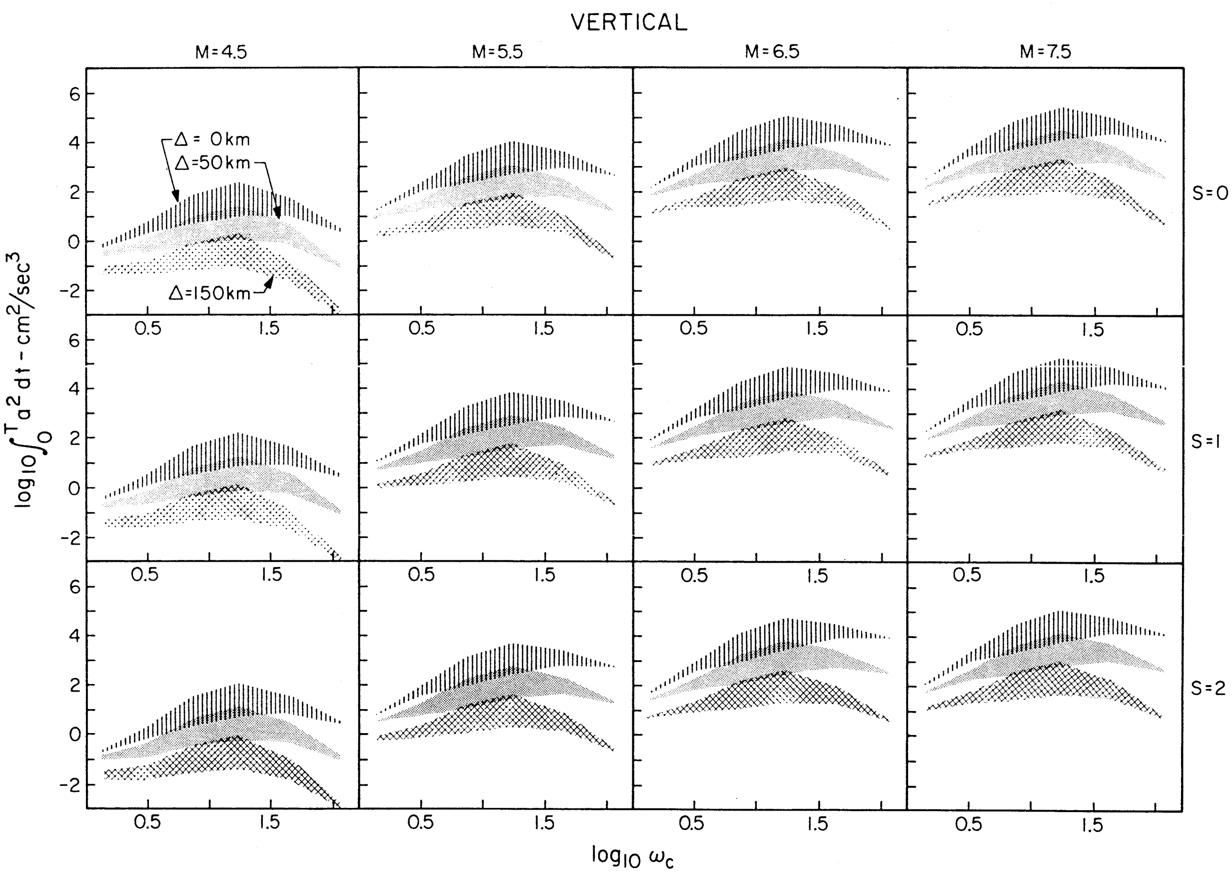

Figure 7a. Amplitudes of $\log_{10} \int_0^T a^2 dt$ for vertical and horizontal motions, different magnitudes, epicentral distances and site conditions [computed from equation (5)].

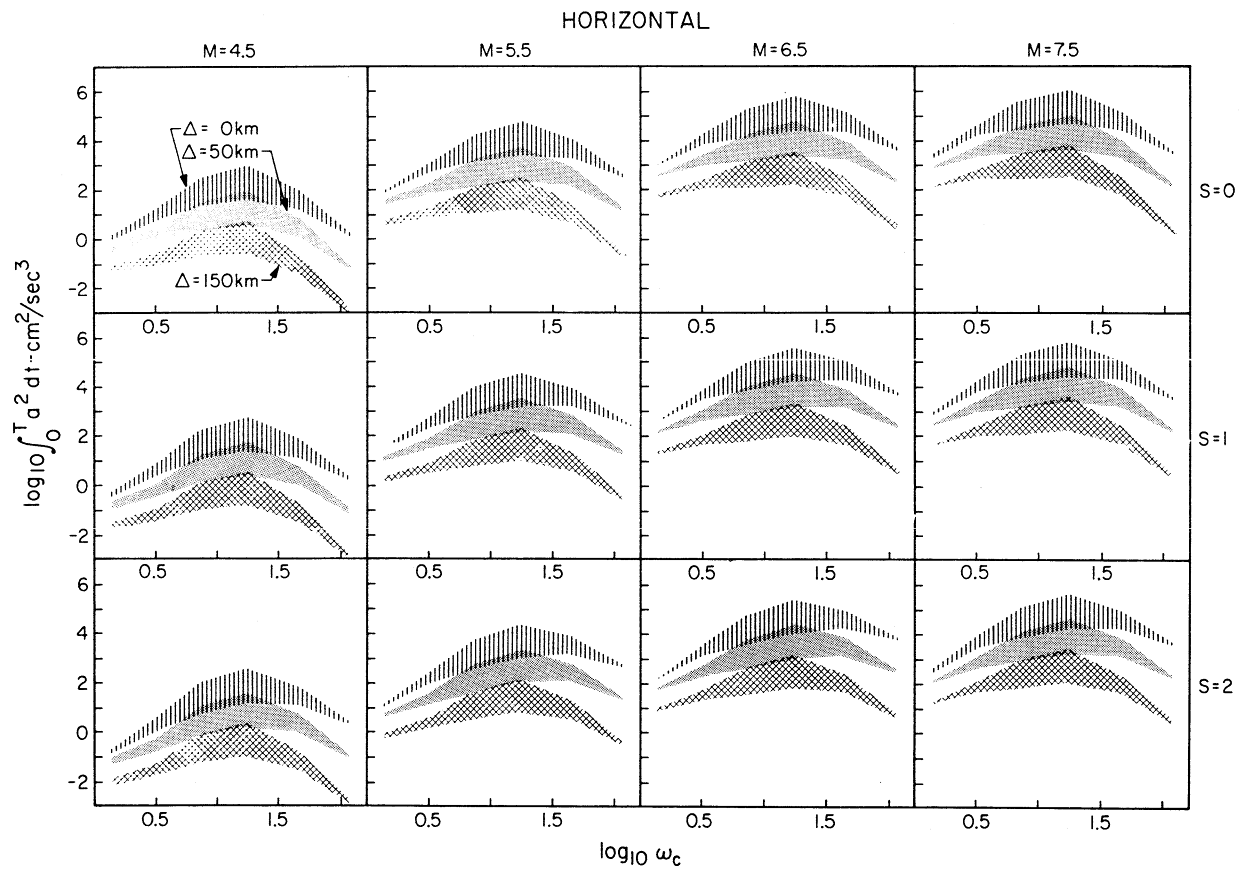

Figure 7b. Amplitudes of $\log_{10} \int_0^T a^2 dt$ for vertical and horizontal motions, different magnitudes, epicentral distances and site conditions [computed from equation (5)].

$\log_{10} \int_0^T a^2 dt$ has been computed from the range of the estimates for the "coefficients" a, b, . . . , e and f in Figure 5 and by using equations (5) and (8). These amplitudes were then smoothed by $\frac{1}{4}, \frac{1}{2}, \frac{1}{4}$ filter along $\log_{10} \omega_c$ axis. These figures show that the largest amplitudes of $\int_0^T a^2 dt$ occur for frequencies near 3 cps ($\omega_c \approx 20$ rad/sec) and that the amplitudes of $\int_0^T a^2 dt$ can be up to several orders of magnitude smaller for the extreme high- and low-frequency bands considered in this study. Other properties of these amplitudes are the same as those we discussed above while explaining the trends of the coefficient functions a, b, c, d, e and f and will not be repeated here.

DEPENDENCE OF THE DURATION OF ACCELERATION, VELOCITY, AND DISPLACEMENT ON FREQUENCY, MAGNITUDE, DISTANCE, AND SITE CONDITIONS

In developing an empirical model to determine the form of the correlations between duration and the parameters which describe the earthquake and the recording site, we are faced with a lack of theoretical work which might indicate the proper functional form for such correlations and thus we consider only a rough approximation suggested by Trifunac and Brady (1975). We assume the total duration of strong motion within a narrow frequency band to be the sum of three contributions as follows,

$$\text{Duration of} \begin{Bmatrix} a \\ v \\ d \end{Bmatrix} = d_s + d_{source} + d_\Delta \ . \tag{14}$$

In equation (14) d_s represents the contribution to the duration caused by the multiple reflections and scattering of the waves by discontinuities along the propagation path and by the surface topography. This term could then be of the form $d_s \propto s + \gamma\Delta$ where γ is some frequency dependent constant. Neglecting higher order and cross product terms involving s and Δ we will assume in this paper that $d_s = a(\omega_c)s$ and will combine the contribution to $d_s \propto \Delta$ with the expression for d_Δ. The second term in (14), d_{source}, represents the contribution to the duration generated at the earthquake source. Although not all earthquakes can be characterized by a dislocation propagating from one end of a fault to the other, an approximation would be to assume this, and thus d_{source} would be proportional to the fault length divided by the dislocation velocity. From the trend of data presented by Thatcher and Hanks (1973), an approximate correlation of earthquake magnitude with fault length, L (in km), would be

$$M \doteq 3 + 2\log_{10} L \, . \tag{15}$$

This suggests that d_{source} could be modeled by $d_{source} \propto 10^{pM}$ where p is a constant to be determined for each frequency band and for horizontal and vertical motions separately.

We did perform a detailed nonlinear regression analysis in which $d_{source} \propto 10^{pM}$ and found that the concentration of the available data points in the magnitude range between $M = 6$ and $M = 7$ resulted in poor control on p and several other regression coefficients. The presence of digitization noise in some low frequency bands (Trifunac 1976b) and serious lack of data points for large magnitudes ($M > 7$) have led us to adopt simpler functional dependence of d_{source} on magnitude of the form

$$d_{source} = bM \tag{16}$$

as an interim approximation in the limited magnitude range for which the data are now available.

Following Trifunac and Brady (1975) we assume that d_Δ, the contribution to duration which results from dispersion of direct arrivals, is a linear function of epicentral distance, Δ, such that

$$d_\Delta = c\Delta \tag{17}$$

where c could be interpreted to mean

$$c = \frac{1}{v_{min}} - \frac{1}{v_{max}} \,. \tag{18}$$

In equation (18) v_{min} and v_{max} are minimum and maximum wave speeds, respectively, for the frequency range considered. Equation (18) could further be expanded to reflect more explicitly the contribution to the duration of shaking that results from repeated reflections and scattering along the propagation path, but these effects may also be thought of as being a part of a more general dispersion model of the propagation path with v_{max} and v_{min} representing the largest and the smallest group velocities for a given frequency band for which c is being computed. It can further be seen that in a more refined model, c in equation (18) would also depend on the site classification s because for the softer surficial layers and alluvium (s = 0) v_{min} would tend to diminish thereby increasing c. To detect such characteristics in an empirical model for the duration of strong shaking it seems that it would be necessary to develop more detailed site classification than what is available to us today in terms of s = 0, 1 and 2 (Trifunac and Brady, 1975), and to have strong motion recordings from more stations in different geologic settings. For these reasons, in this paper we will consider only one of the simplest empirical models for the duration of strong shaking by neglecting the dependence of c on the recording site conditions and will assume that v_{min} and v_{max} in (18) then reflect the overall averages for all stations where the data employed in this paper have been recorded.

Based on the discussion above we consider the following approximate model for the frequency dependent model of the duration of strong ground motion,

$$\text{Duration of} \begin{Bmatrix} a \\ v \\ d \end{Bmatrix} = as + bM + c\Delta + d \ . \qquad (19)$$

Table IV presents the results of the regression analysis for acceleration, velocity, and displacement of both horizontal and vertical components and for the six frequency bands.

If we assume that the band-pass filtered motions may be approximated by the center frequency of each band, we see that for a component of motion with a given frequency band

$$\text{Duration of } \{a\} \doteq \text{Duration of } \{v\} \doteq \text{Duration of } \{d\} \ . \qquad (20)$$

Therefore, the data in Table IV can be averaged to improve the reliability of the individual estimates. Figure 8 shows the estimated range for each of the coefficients a, b, c and d for acceleration, velocity, and displacement versus the center frequency of each band. These amplitudes for both the horizontal and vertical components of motion are bounded by

TABLE IV

Regression Coefficients in the Duration of

$$\begin{Bmatrix} a \\ v \\ d \end{Bmatrix} = as + bM + c\Delta + d \pm \sigma; \quad \sigma = A + B\Delta \pm \Sigma$$

VERTICAL ACCELERATION

Center Frequency	f_c = 18.0	f_c = 7.0	f_c = 2.8	f_c = 1.1	f_c = 0.5	f_c = 0.2
a	-1.04	-1.23	-3.30	-5.83	-6.80	-4.45
b	.34	1.38	2.12	.51	-.47	-1.09
c	.12	.08	.08	.08	.06	.08
d	3.43	-.57	-.95	16.16	29.57	30.62
σ	5.34	4.59	5.93	8.86	11.65	12.44
A	1.38	1.72	2.81	5.36	8.43	9.34
B	.03	.02	.02	.02	.02	.01
Σ	3.82	3.11	4.13	5.55	6.77	7.44
No. of Data	180	180	180	180	180	180

VERTICAL VELOCITY

a	-.99	-1.36	-3.64	-5.96	-6.13	-5.24
b	.53	1.52	2.14	-.06	.20	-1.15
c	.13	.08	.08	.08	.06	.08
d	2.09	-1.16	.08	20.37	23.96	32.17
σ	5.07	4.44	6.38	8.83	11.36	12.95
A	1.18	1.68	3.53	5.73	8.10	9.81
B	.04	.02	.02	.02	.02	.01
Σ	3.38	3.03	4.38	5.46	6.51	7.28
No. of Data	180	180	180	180	180	180

VERTICAL DISPLACEMENT

a	-3.73	-1.49	-3.95	-5.71	-6.18	-5.06
b	.36	1.59	1.79	.44	.27	-1.37
c	.15	.08	.08	.08	.07	.08
d	9.63	-1.33	3.16	17.95	23.45	34.92
σ	10.01	4.51	6.78	9.41	11.81	13.09
A	4.81	1.81	3.79	6.09	8.51	9.97
B	.05	.02	.02	.02	.02	.01
Σ	6.10	3.05	4.56	5.65	6.85	7.53
No. of Date	180	180	180	180	180	180

TABLE IV (Concluded)

HORIZONTAL ACCELERATION

Center Frequency	f_c = 18.0	f_c = 7.0	f_c = 2.8	f_c = 1.1	f_c = 0.5	f_c = 0.2
a	-1.66	-1.38	-2.75	-4.09	-4.82	-3.02
b	.64	1.32	1.28	-.36	1.68	-.43
c	.13	.08	.09	.08	.07	.09
d	1.88	-.77	1.42	16.41	11.82	22.00
σ	5.89	5.10	5.57	7.41	10.75	12.01
A	1.92	1.94	2.67	4.60	7.13	8.74
B	.04	.03	.02	.02	.02	.02
Σ	3.90	3.40	3.65	4.66	6.46	6.79
No. of Data	360	360	360	360	360	360

HORIZONTAL VELOCITY

a	-1.76	-1.28	-2.86	-3.99	-4.69	-3.38
b	.61	1.50	1.14	-.19	-.06	-1.79
c	.13	.07	.09	.08	.07	.08
d	2.13	-1.62	2.78	15.95	23.19	32.07
σ	5.93	4.96	5.56	7.91	10.96	12.27
A	1.95	1.98	2.71	5.02	7.50	9.67
B	.04	.03	.02	.02	.02	.01
Σ	3.97	3.20	3.48	4.95	6.44	7.03
No. of Data	360	360	360	360	360	360

HORIZONTAL DISPLACEMENT

a	-5.00	-1.41	-3.02	-4.54	-4.68	-3.45
b	1.46	1.47	.87	.14	1.01	-1.34
c	.12	.07	.09	.08	.07	.08
d	5.30	-1.21	4.88	15.17	16.58	29.82
σ	10.54	4.92	5.97	8.35	11.19	11.90
A	5.00	2.18	2.83	5.13	7.70	9.46
B	.05	.02	.03	.02	.02	.003
Σ	6.82	3.20	3.80	5.19	6.52	6.97
No. of Data	360	360	360	360	360	360

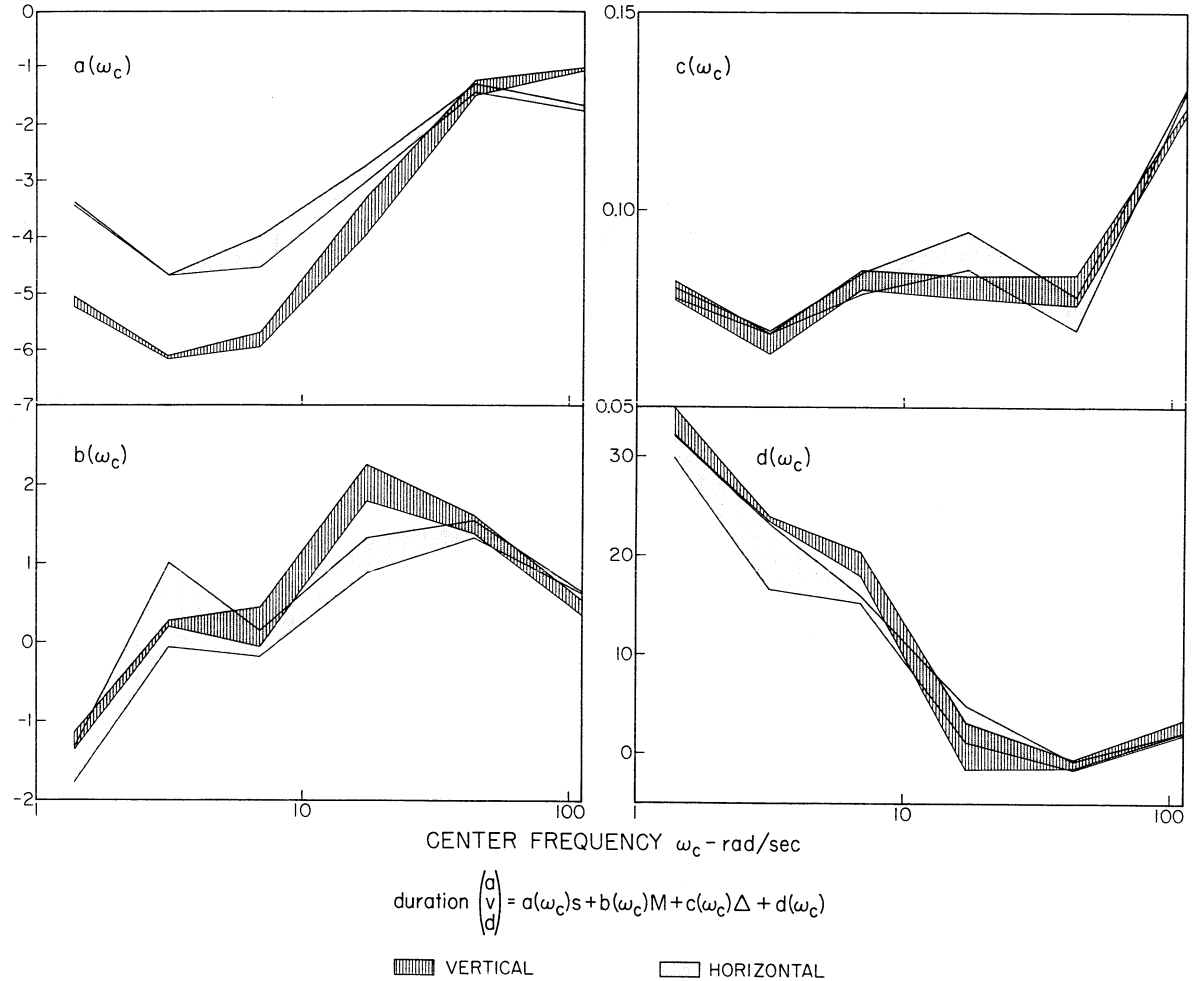

Figure 8. Coefficients a, b, c and d in equation (19) for horizontal and vertical components, plotted versus $\omega_c = 2\pi f_c$ (for $f_c = 0.2, 0.5, 1.1, 2.7, 7.0$ and 18.0).

the mean plus and minus the maximum difference between the mean and the extreme values of the coefficients for acceleration, velocity, or displacement. For the same reasons as in the previous section, the values for coefficients derived from data with a low signal-to-noise ratio, high frequency displacements (band no. 1), and low frequency accelerations (bands no. 4, 5 and 6) were not used in computing the "coefficients" a through d in Figure 8.

From Figure 8 it can be seen that, because $a < 0$, the general trend of the duration is to decrease for "harder" sites ($s = 2$) in all the frequency bands studied. For high frequencies it decreases by about 3 to 4 seconds and at lower frequencies the duration decreases by 9 to 12 seconds in going from a "soft" ($s = 0$) site to a "hard" ($s = 2$) site. We interpret this to result from more discontinuities and irregularities underneath the "soft" sites which lead to stronger scattering of the waves in the vicinity of the recording station and thus lengthen the duration.

The curve representing the correlation parameter c versus $\omega_c = 2\pi f_c$ (Figure 8) shows c to be almost constant except at the highest frequency band ($f_c = 18.0$ cps). The increase of c at this band indicates a larger difference between the maximum and minimum wave speeds at high frequencies. The average value of about 0.08 for c for low frequencies yields $v_{max} \doteq 4$ km/sec in equation (18) assuming, for example, $v_{min} = 3$ km/sec. For the high frequency average of c of about 0.13, equation (18) yields $v_{max} \doteq 5.0$ km/sec with $v_{min} = 3$ km/sec.

A marked change in the behavior of the curves representing b (Figure 8) appears at the frequency band near $f_c = 1.1$ cps. For the data within and below this frequency band the nature of the correlation changes, and the duration term d_{source} ceases to depend on or begins to decrease with an increase in magnitude. This shift in the behavior of bM appears to result from low signal-to-noise ratio for the data at the low frequency end of the spectrum. What this means is that a low magnitude earthquake would produce waves of low frequency which would appear to have a long duration because these wave amplitudes would be contaminated by signal processing noise. A larger earthquake would produce the same "noisy" waves but also a much larger amplitude group of near-field and body waves with a shorter duration. Thus, by our definition of duration, we would observe a tendency for duration to decrease with an increase in magnitude for those frequency bands which are characterized by low or poor signal-to-noise ratio and the opposite trend for the frequency bands which are characterized by good signal-to-noise ratios (Trifunac, 1976b).

Because of the relatively stronger scattering of high frequency waves, compared to longer waves, it would be expected that the scatter of data about the proposed correlation equation would increase with distance and that this increase would be greatest for the high frequency waves. Table IV, which shows the coefficients A and B and the standard deviation Σ for the regression

$$\sigma = A + B\Delta \pm \Sigma , \tag{21}$$

shows that this is indeed the case.

If the data on durations were available for motions at the source ($\Delta = 0$), it would be expected that the total duration of motion would correspond to the duration of faulting (neglecting any extraneous site effects). At large distances the duration would be extended mainly by the dispersion of the waves. Figures 9a and 9b show the averaged durations calculated from the coefficients in equation (19) versus $\log_{10}\omega_c$ for various values of magnitude, distance, and site conditions and for both the horizontal and vertical components. These curves were filtered along the $\log_{10}\omega_c$ axis by $\frac{1}{4}, \frac{1}{2}, \frac{1}{4}$ filter to show the smooth trends of the duration with the variables considered. For a "hard site" ($s = 2$) and $\Delta = 0$ the duration for the high frequency bands ranges from several seconds for a magnitude of 4.5 to 5 to 10 seconds for a magnitude of 7.5. This would roughly correspond to the duration of faulting.

For the studies which examine the damaging potential of strong earthquake ground motion and analyze nonlinear response of progressively weakening structures, it may be useful to consider the number of cycles a linear elastic oscillator may be expected to experience during a time interval which we call the duration of strong ground motion. This number of cycles, equal to the product of the natural frequency of an oscillator, f_n, and the corresponding duration, has been plotted in Figures 10a and 10b versus $\log_{10}\omega_c$ and for different magnitudes, site conditions and epicentral distances. It is seen from these figures that

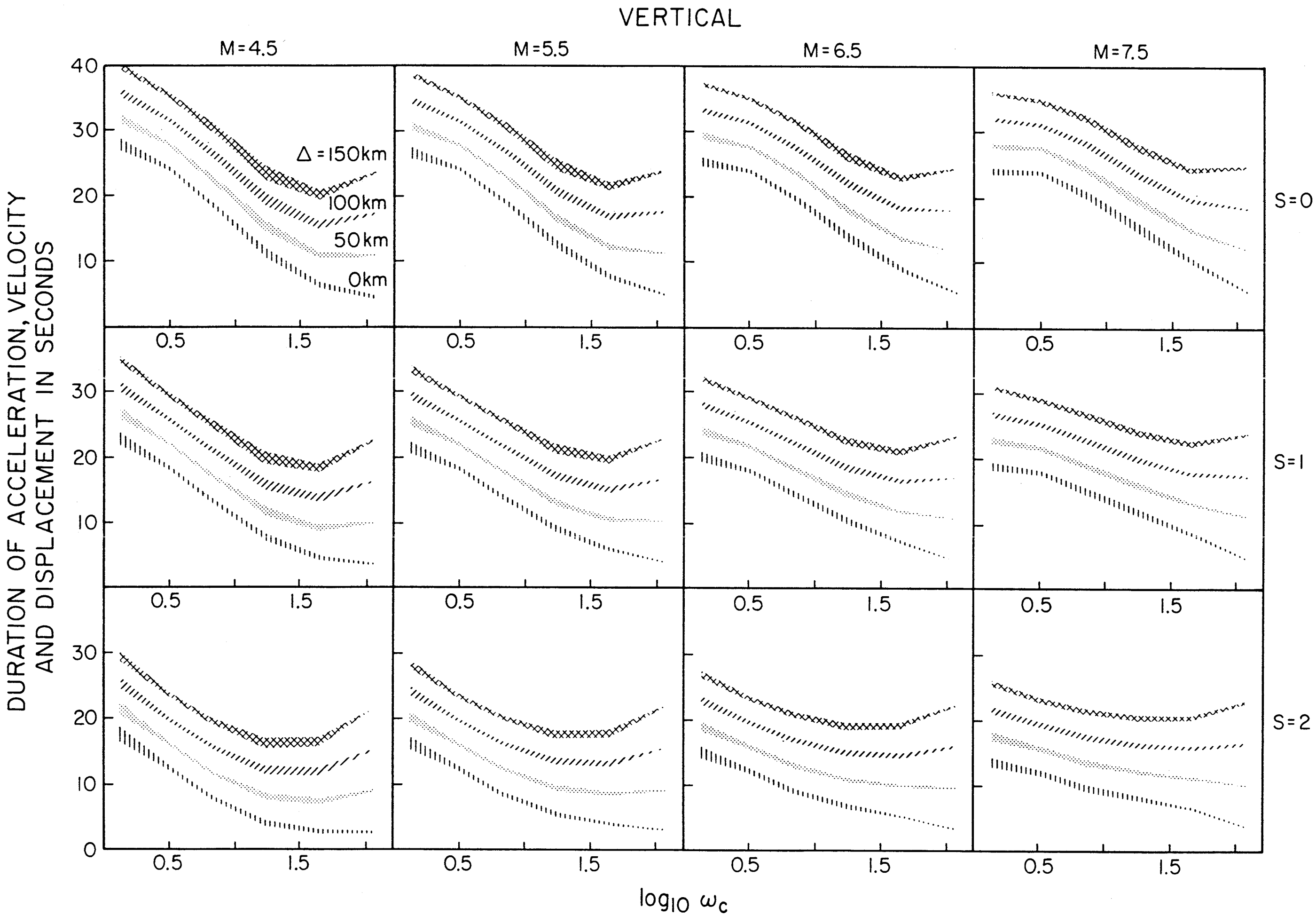

Figure 9a. The duration of vertical strong ground motion as calculated from equation (19) versus frequency, magnitude, epicentral distance, and site conditions.

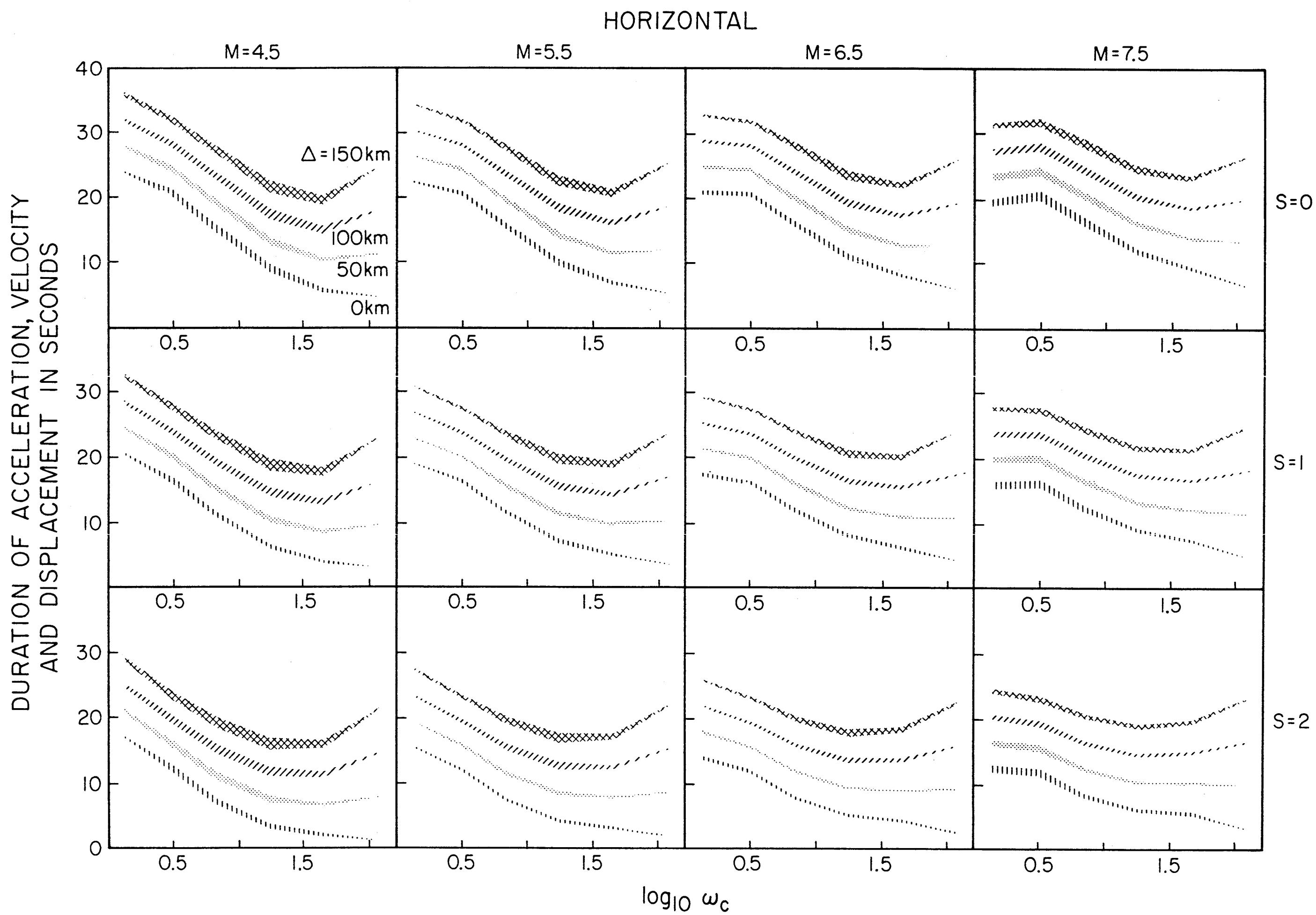

Figure 9b. The duration of horizontal strong ground motion as calculated from equation (19) versus frequency, magnitude, epicentral distance, and site conditions.

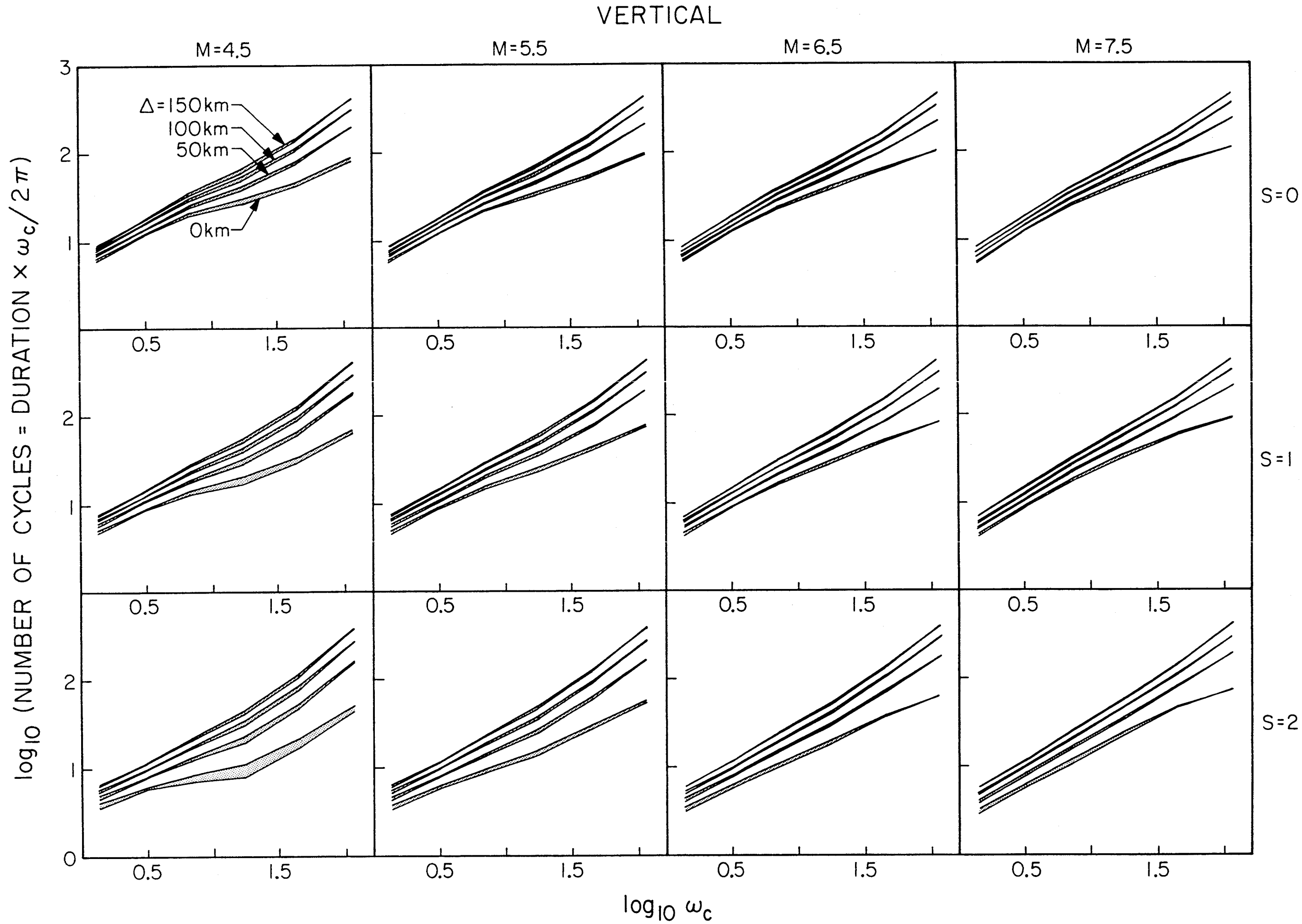

Figure 10a. The number of cycles of vibration for a single degree-of-freedom oscillator for the duration of shaking expressed by equation (19).

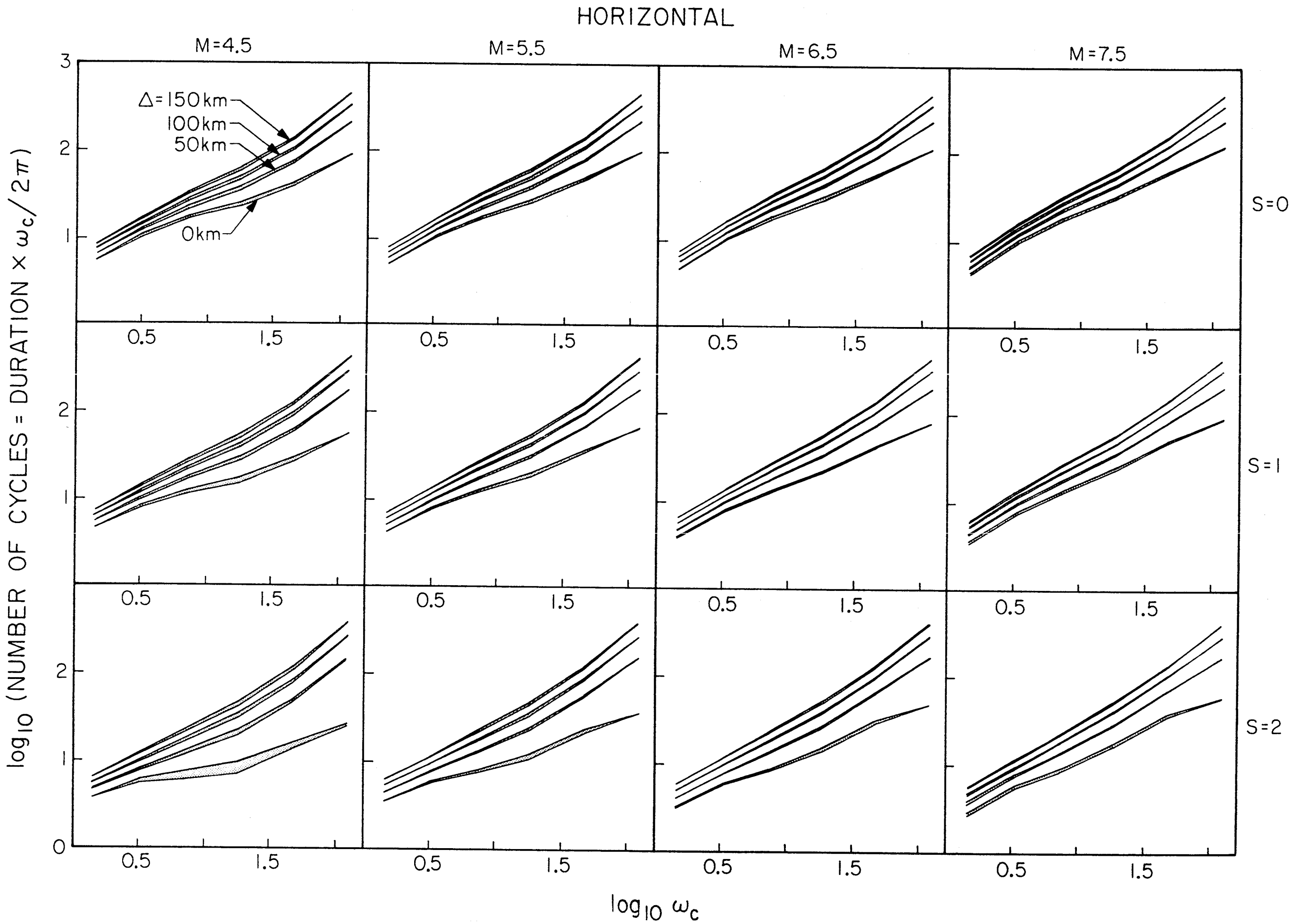

Figure 10b. The number of cycles of vibration for a single degree-of-freedom oscillator for the duration of shaking expressed by equation (19).

the number of cycles varies from less than ten for $f_c = 0.2$ cps to about 500 for $f_c = 18$ cps and that the most prominent factor which increases the number of cycles is the epicentral distance Δ. For moderate and high frequencies the number of cycles increases with magnitude and decreases from alluvium (s = 0) to hard rock sites (s = 2) but these changes are small compared to the changes with epicentral distance.

CORRELATIONS OF THE "POWER" OF STRONG GROUND MOTION WITH MAGNITUDE, SITE CONDITIONS, AND EPICENTRAL DISTANCE

As mentioned in the earlier discussion, the average time rates of growth of the integrals $\int_0^t \begin{Bmatrix} a^2 \\ v^2 \\ d^2 \end{Bmatrix} d\tau$ could be useful for the response analysis of nonlinear yielding structures to strong ground motion. For example, the power or average rate of energy input into a structure is proportional to $\int_0^t a^2 dt/\text{duration}$ and thus represents the power available for damage. Defining the average rate by

$$\text{Rate} \equiv \int_0^T \begin{Bmatrix} a^2 \\ v^2 \\ d^2 \end{Bmatrix} dt/\text{duration of strong motion} \tag{22}$$

an estimate of this quantity could be calculated from equations (5) and (19). To avoid cumulative errors, which might result from previous assumptions, new correlations have been performed by using

$$\log_{10}\left[\int_0^T \begin{Bmatrix} a^2 \\ v^2 \\ d^2 \end{Bmatrix} dt \Big/ \text{duration}\right] = as + bM + c\Delta + e\log_{10}A_0(\Delta) + fM^2 + d \quad . \; (23)$$

$$, \; M \leq M_{max}$$

Table V gives the values of the coefficients in equation (23) for horizontal and vertical components of acceleration, velocity, and displacement and for all six frequency bands. As in the correlations of $\int_0^T \begin{Bmatrix} a^2 \\ v^2 \\ d^2 \end{Bmatrix} dt$ with s, M and Δ, if we assume the frequency bands to be narrow enough, then the coefficients in Table V can be combined in exactly the same manner as for the data in Table III. Figure 11 presents these coefficients for acceleration. The velocity and displacement coefficients would all be expected to be the same, with the exception of the coefficient d, as already explained [see equation (8)] in the earlier analysis of $\int_0^T \begin{Bmatrix} a^2 \\ v^2 \\ d^2 \end{Bmatrix} dt$.

The influence of site conditions on the average rate and on $\int_0^T \begin{Bmatrix} a^2 \\ v^2 \\ d^2 \end{Bmatrix} dt$ is similar because of the stronger dependence of $\int_0^T \begin{Bmatrix} a^2 \\ v^2 \\ d^2 \end{Bmatrix} dt$ on the site condition than the dependence of duration on the same conditions. For low frequencies a "hard" site (s = 2) leads to the rate which is about 5 times smaller than the same at a "soft" site (s = 0), but at high frequencies a "hard" site leads to rate typically 1.5 times larger than the rate at "soft" sites.

TABLE V

Regression Coefficients for

$$\log_{10}\left\{\int_0^T \begin{pmatrix} a^2 \\ v^2 \\ d^2 \end{pmatrix} dt/\text{duration}\right\} = as + bM + c\Delta + e\log_{10}A_0(\Delta) + fM^2 + d \pm \sigma$$

$$M \leq M_{max}$$

$$\sigma = A + B\log_{10}\Delta \pm \Sigma$$

VERTICAL ACCELERATION

	f_c = 18.0	f_c = 7.0	f_c = 2.7	f_c = 1.1	f_c = 0.5	f_c = 0.2
a	.072	-.033	-.009	-.064	-.137	-.179
b	8.08	6.68	4.61	5.45	5.71	4.79
c	-.0123	-.0104	-.0048	-.0011	-.0002	-.0085
d	-18.1	-19.3	-12.5	-16.0	-17.8	-17.0
e	0.99	0.71	0.86	1.10	1.08	.08
f	-.58	-.47	-.32	-.36	-.37	-.31
σ	.68	.55	.50	.52	.64	.68
A	.56	.44	.44	.52	.64	.66
B	-.0007	-.0004	-.0010	-.0018	-.0023	-.0017
Σ	.44	.35	.32	.30	.38	.37
No. of Data	180	180	180	180	180	180
M_{max}	6.98	7.03	7.29	7.49	7.63	7.72

VERTICAL VELOCITY

	f_c = 18.0	f_c = 7.0	f_c = 2.7	f_c = 1.1	f_c = 0.5	f_c = 0.2
a	.060	-.038	-.023	-.084	-.156	-.115
b	8.15	6.37	4.33	5.51	5.59	4.64
c	-.0125	-.0099	-.0042	-.0010	-.0014	-.0089
d	-22.3	-21.5	-14.1	-17.9	-18.5	-16.6
e	.94	.69	.85	1.12	.95	-.04
f	-.59	-.45	-.29	-.36	-.37	-.31
σ	.67	.54	.49	.51	.66	.64
A	.54	.44	.45	.51	.66	.61
B	-.0005	-.0005	-.0010	-.0017	-.0022	-.0015
Σ	.43	.35	.31	.30	.38	.37
No. of Data	180	180	180	180	180	180
M_{max}	6.94	7.05	7.38	7.55	7.64	7.49

TABLE V (Continued)

VERTICAL DISPLACEMENT

	f_c = 18.0	f_c = 7.0	f_c = 2.7	f_c = 1.1	f_c = 0.5	f_c = 0.2
a	.077	-.042	-.005	-.083	-.136	-.149
b	8.12	6.26	3.66	4.94	5.24	4.47
c	-.0049	-.0095	-.0037	-.0018	-.0026	-.0082
d	-25.3	-24.1	-14.4	-17.8	-18.3	-16.2
e	1.39	.69	.84	1.02	.81	-.05
f	-.58	-.44	-.24	-.32	-.34	-.30
σ	.66	.54	.49	.51	.67	.60
A	.59	.45	.44	.51	.65	.56
B	-.0014	-.0006	-.0010	-.0017	-.0020	-.0014
Σ	.42	.35	.30	.30	.39	.35
No. of Data	180	180	180	180	180	180
M_{max}	6.97	7.04	7.68	7.72	7.64	7.49

HORIZONTAL ACCELERATION

	f_c = 18.0	f_c = 7.0	f_c = 2.7	f_c = 1.1	f_c = 0.5	f_c = 0.2
a	.151	.043	-.028	-.144	-.303	-.392
b	9.52	9.08	5.38	5.23	6.16	6.12
c	-.0134	-.0124	-.0064	-.0007	.0030	-.0076
d	-22.5	-26.1	-14.0	-14.4	-17.9	-20.0
e	.81	.58	.88	1.21	1.42	.34
f	-.71	-.68	-.38	-.34	-.41	-.41
σ	.72	.60	.53	.58	.64	.80
A	.60	.46	.47	.58	.59	.80
B	-.0011	-.0001	-.0012	-.0021	-.0016	-.0024
Σ	.47	.40	.34	.34	.40	.44
No. of Data	360	360	360	360	360	360
M_{max}	6.73	6.69	7.12	7.59	7.52	7.42

HORIZONTAL VELOCITY

	f_c = 18.0	f_c = 7.0	f_c = 2.7	f_c = 1.1	f_c = 0.5	f_c = 0.2
a	.146	.025	-.065	-.178	-.326	-.348
b	9.48	8.69	5.29	5.28	6.69	6.01
c	-.0137	-.0116	-.0055	-.0003	.0009	-.0086
d	-26.3	-27.9	-16.1	-16.1	-21.1	-20.4
e	.75	.62	.91	1.25	1.19	.18
f	-.70	-.65	-.37	-.35	-.45	-.40
σ	.72	.59	.52	.61	.64	.79
A	.60	.46	.46	.61	.59	.80
B	-.0011	-.0003	-.0012	-.0024	-.0014	-.0024
Σ	.48	.39	.33	.36	.39	.43
No. of Data	360	360	360	360	360	360
M_{max}	6.72	6.72	7.17	7.60	7.48	7.50

TABLE V (Concluded)

HORIZONTAL DISPLACEMENT

	f_c = 18.0	f_c = 7.0	f_c = 2.7	f_c = 1.1	f_c = 0.5	f_c = 0.2
a	.103	.014	-.099	-.151	-.338	-.358
b	7.73	8.79	5.32	5.08	6.09	6.15
c	-.0045	-.0107	-.0045	-.0005	.0010	-.0091
d	-24.4	-31.1	-18.4	-17.2	-20.0	-20.7
e	1.14	.68	.97	1.20	1.22	.07
f	-.55	-.66	-.37	-.33	-.40	-.42
σ	.63	.60	.53	.59	.66	.75
A	.53	.48	.47	.60	.63	.74
B	-.0012	-.0004	-.0013	-.0022	-.0018	-.0021
Σ	.42	.39	.34	.34	.39	.41
No. of Data	360	360	360	360	360	360
M_{max}	6.98	6.71	7.16	7.68	7.59	7.26

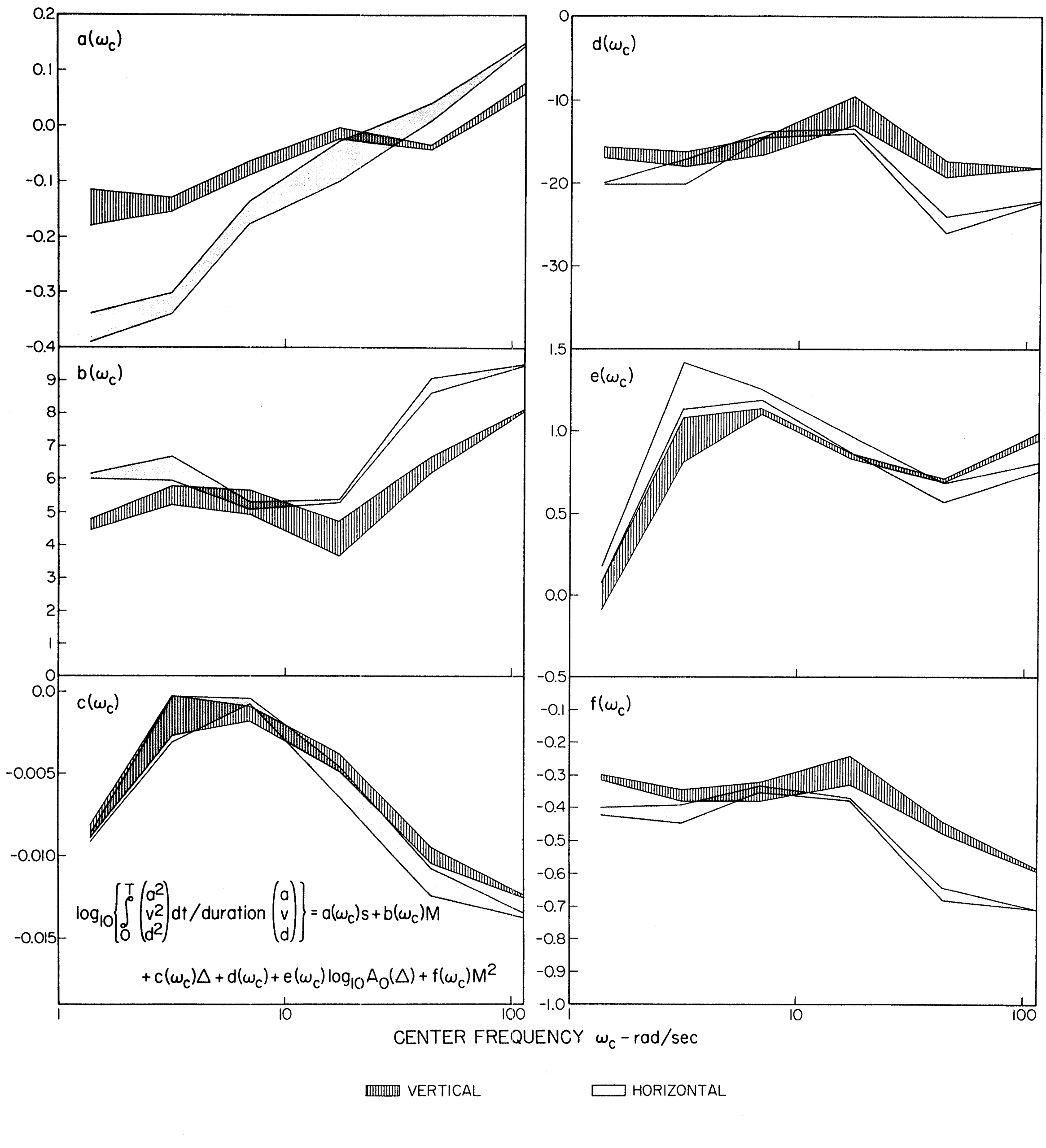

Figure 11. Coefficients a, b, c, d, e and f in equation (23) for horizontal and vertical components of acceleration, plotted versus $\omega_c = 2\pi f_c$ (for $f_c = 0.2$, 0.5, 1.1, 2.7, 7.0 and 18.0). Corresponding results for velocity and displacement can be obtained from equation analogous to equations (8).

The dependence of the rate on epicentral distance (Figure 11) is also similar to the dependence of $\log_{10} \int_0^T \begin{Bmatrix} a^2 \\ v^2 \\ d^2 \end{Bmatrix} dt$ on distance. The high frequency rate is most highly reduced with distance probably because of the stronger attenuation of high frequency waves and the large dispersion.

The nature of the increase of the rate with an increase in earthquake magnitude is nearly the same for all the frequency bands. As with the correlations for

$\int_0^T \begin{Bmatrix} a^2 \\ v^2 \\ d^2 \end{Bmatrix} dt$, for magnitudes larger than M_{max}, the magnitudes at which the peaks of $bM + fM^2$ occur, we define

$$\log_{10}\left[\int_0^T \begin{Bmatrix} a^2 \\ v^2 \\ d^2 \end{Bmatrix} dt \Big/ \text{duration}\right] = as + bM_{max} + c\Delta + e\log_{10} A_0(\Delta) + fM_{max}^2 + d \ .$$

$$\text{for } M \geq M_{max} \qquad (24)$$

Figure 12 shows that the rate increases by as much as 10^3 times (on the linear scale) for a magnitude 7.5 earthquake compared to magnitude 4.5.

As in the previous analysis of $\log_{10} \int_0^T \begin{Bmatrix} a^2 \\ v^2 \\ d^2 \end{Bmatrix} dt$, the scatter of data with respect to equation (29) has been correlated with distance by

$$\sigma = A + B \log_{10}\Delta \pm \Sigma \ . \qquad (25)$$

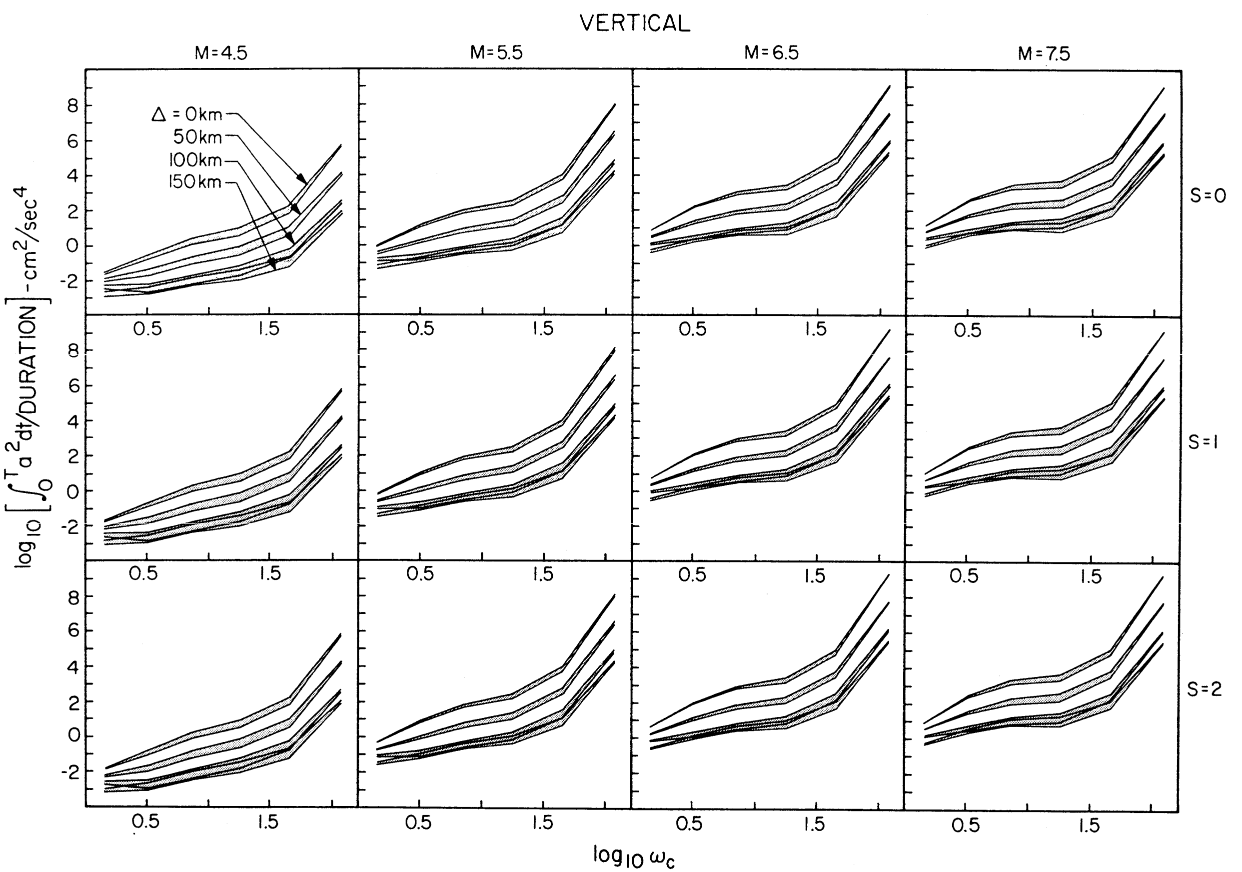

Figure 12a. Amplitudes of $\log_{10} \int_0^T a^2 dt/\text{duration}$ for vertical and horizontal motions, different magnitudes, epicentral distances and site conditions [computed from equation (23)].

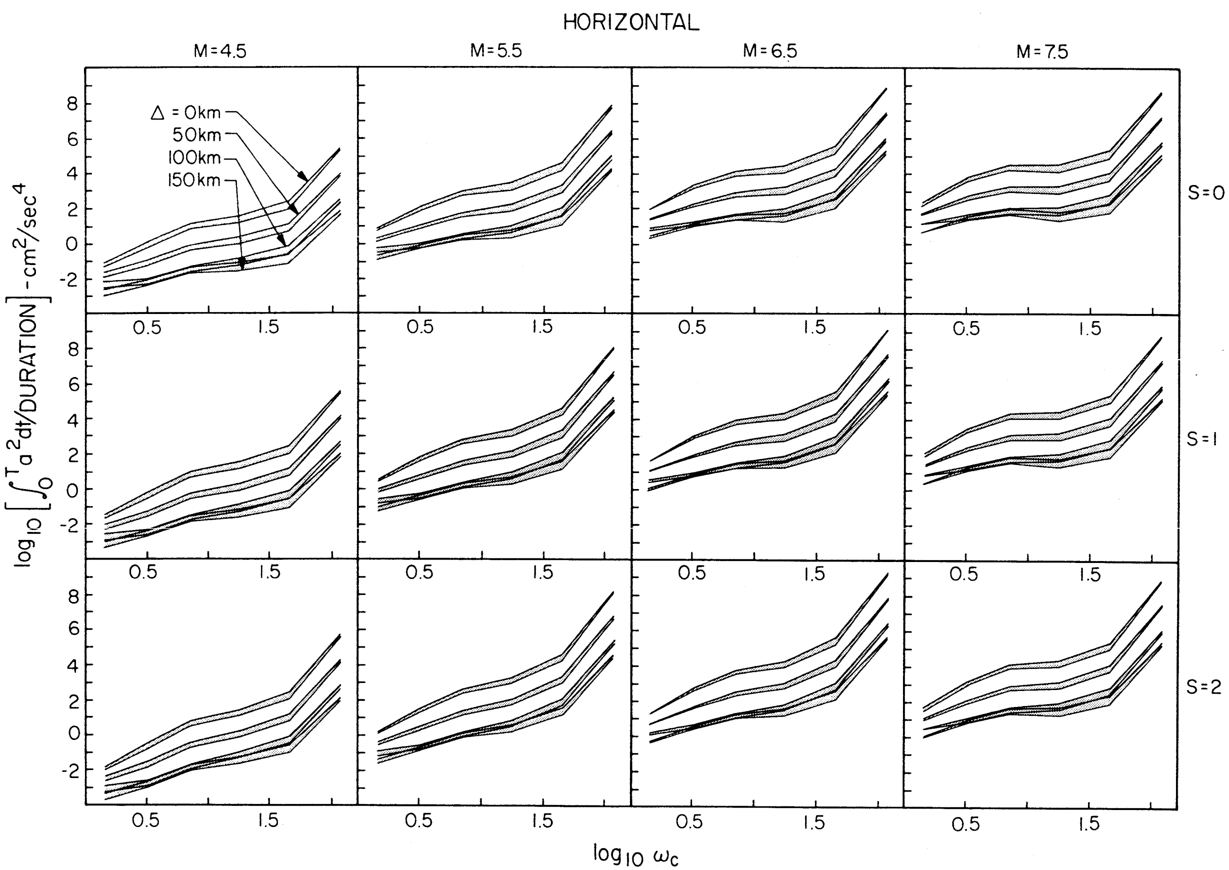

Figure 12b. Amplitudes of $\log_{10} \int_0^T a^2 dt/\text{duration}$ for vertical and horizontal motions, different magnitudes, epicentral distances and site conditions [computed from equation (23)].

The coefficients A, B and standard deviation, Σ, in Table V show the quality of fit again bettering with an increase in distance Δ.

Figures 12a and 12b present a summary of the dependence of $\log_{10}$ (rate of growth of $\int_0^t f^2 d\tau$) ($\propto$ power of $\int_0^T a^2 dt$) on magnitude, site conditions and epicentral distance plotted versus $\log_{10} \omega_c$. It can be seen from these figures that the rate increases more rapidly for frequencies higher than about 5 to 10 cps and that the epicentral distance, Δ, is the most prominent factor which influences its amplitudes. The effects of magnitude and site conditions can be seen to be less important.

CONCLUSIONS

The results of the analysis in this study depend on the definitions and assumptions which were employed in the formulation of the approximate models for $\int_0^T \begin{Bmatrix} a^2 \\ v^2 \\ d^2 \end{Bmatrix} dt$, duration, and the time rate of growth of these integrals in terms of earthquake magnitude, distance, and recording site conditions. The correlation equations used represent only rough approximations to as yet unknown exact functional relations that may exist among these quantities. The models which we employed are based on the limited knowledge of the phenomena involved, and thus the reliability of the information inferred cannot be extended beyond the range in which this analysis applies.

From the studies of $\log_{10} \int_0^T \begin{Bmatrix} a^2 \\ v^2 \\ d^2 \end{Bmatrix} dt$ we found that the effects of site condition are most predominant at low frequencies with a "soft" site yielding about 7 times larger values of $\int_0^T \begin{Bmatrix} a^2 \\ v^2 \\ d^2 \end{Bmatrix} dt$ than a "hard" site, the horizontal component of motion typically being affected more by the site conditions. The increase in the amplitudes of $\int_0^T \begin{Bmatrix} a^2 \\ v^2 \\ d^2 \end{Bmatrix} dt$ with increasing magnitude is about 1.5 times greater for high frequency motions than it is for low frequencies. For high frequencies $\int_0^T \begin{Bmatrix} a^2 \\ v^2 \\ d^2 \end{Bmatrix} dt$ is about 10^4 times larger for magnitude M = 7.0 than for magnitude M = 4.5. For low frequencies $\int_0^T \begin{Bmatrix} a^2 \\ v^2 \\ d^2 \end{Bmatrix} dt$ is about 10^3 to 10^4 times larger for magnitude M = 7.0 than for the magnitude M = 4.5. The amplitudes of $\int_0^T \begin{Bmatrix} a^2 \\ v^2 \\ d^2 \end{Bmatrix} dt$ decrease with increasing distance, Δ, because of attenuation and geometric spreading. This attenuation is most prominent for high frequencies with the integral amplitudes reduced by a factor of about 0.8 with each increase of 10 km.

The dependence of duration on site conditions is most prominent for the lower frequencies with a decrease in duration of as much as 9 to 12 seconds for a "hard" site (s = 2) compared to a "soft" site (s = 0).

The duration does not vary by more than about 3 seconds in this respect for high frequency strong motion. For the assumed linear dependence of duration on magnitude it has been found that for high frequencies (f_c = 18.0 cps) the duration increases by less than 3 seconds for a magnitude M = 7.5 earthquake compared to a magnitude M = 4.5 earthquake while for the frequency band f_c = 2.75 cps this increase is about 6 seconds. Inferences about the low frequency data could not be derived because of the presence of noise in the data for frequencies lower than about 1 cycle per second. For frequencies lower than about 7 cycles per second the duration increases by about 0.7 seconds for every 10 km of distance, while for the high frequencies it increases by as much as 1.4 seconds for every 10 km increase in distance.

The correlations of $\int_0^T \begin{Bmatrix} a^2 \\ v^2 \\ d^2 \end{Bmatrix} dt/\text{duration}$ with magnitude, epicentral distance, and site conditions for the six frequency bands lead to the behavior similar to that for $\int_0^T \begin{Bmatrix} a^2 \\ v^2 \\ d^2 \end{Bmatrix} dt$. The rate at "soft" sites for low frequency motion is about six times larger than for "hard" sites, while for high frequencies the "soft" site amplitude of the rate is about two times less than for "hard" sites. The attenuation of the rate with distance is most pronounced for high frequencies because of the greater attenuation at high frequencies of $\int_0^T \begin{Bmatrix} a^2 \\ v^2 \\ d^2 \end{Bmatrix} dt$ and the increase of duration from the larger dispersion at high frequencies.

When more recorded data becomes available for analysis, it should be possible to carry out more detailed investigations and make better inferences about the models and the related parameters which characterize the duration of strong ground motion. Meanwhile, the correlations presented in this paper may prove to be useful in seismological and engineering investigations provided that it is remembered that these results are of preliminary nature and are limited by the number and range of the available data.

ACKNOWLEDGMENTS

We are grateful to J. G. Anderson and J. E. Luco for critical reading of the text and numerous useful suggestions which led to several important improvements in this paper.

Significant parts of this research were supported by contracts from the U.S. Geological Survey and the Nuclear Regulatory Commission and by the Earthquake Research Affiliates Program at the California Institute of Technology while the senior author was a member of the Earthquake Engineering Research Laboratory there. This work was completed at the University of Southern California with support from the Nuclear Regulatory Commission. All financial assistance is gratefully acknowledged.

Department of Civil Engineering
University of Southern California
University Park
Los Angeles, California 90007
(M. D. Trifunac)

Department of Engineering and Applied Science
California Institute of Technology
Pasadena, California 91125
(B. D. Westermo)

REFERENCES

Arias, A. (1970). A measure of earthquake intensity, in Seismic Design of Nuclear Power Plants, Hansen (ed.), p. 438.

Bolt, B. A. (1973). Duration of strong ground motion, Proc. Fifth World Conf. on Earthquake Engineering, Rome, 6-D, Paper No. 292.

Cartwright, D. E. and M. S. Longuet-Higgins (1956). The statistical distribution of the maxima of a random function, Proc. Roy. Soc. London, Ser. A, 237, 212-232.

Gutenberg, B. and C. F. Richter (1942). Earthquake magnitude, intensity, energy and acceleration, Bull. Seism. Soc. Amer., 32, 163-191.

Gutenberg, B. and C. F. Richter (1956). Earthquake magnitude, intensity, energy, and acceleration, Paper II, Bull. Seism. Soc. Amer., 46, 105-195.

Housner, G. W. (1965). Intensity of ground shaking near the causative fault, Proc. Third World Conf. on Earthquake Engineering, New Zealand, 3, 94-109.

Richter, C. F. (1958). Elementary seismology, Freeman & Co., San Francisco.

Thatcher, W. and T. C. Hanks (1973). Source parameters of Southern California earthquakes, J. Geoph. Res., 78, 8547-8576.

Trifunac, M. D., F. E. Udwadia, and A. G. Brady (1973). Analysis of errors in digitized strong-motion accelerograms, Bull. Seism. Soc. Amer., 63, 157-187.

Trifunac, M. D. and V. W. Lee (1973). Routine computer processing of strong motion accelerograms, Earthquake Engr. Res. Lab., EERL Report No. 73-03, Calif. Inst. of Tech., Pasadena.

Trifunac, M. D. and A. G. Brady (1975). A study on the duration of strong earthquake ground motion, Bull. Seism. Soc. Amer., 65, 581-626.

Trifunac, M. D. (1976a). Preliminary statistical analysis of the peaks of strong earthquake ground motion - dependence of peaks on earthquake magnitude, epicentral distance and recording site conditions, Bull. Seism. Soc. Amer., 66, 189-219.

Trifunac, M. D. (1976b). Preliminary empirical model for scaling Fourier amplitude spectra of ground acceleration in terms of earthquake magnitude, source to station distance, and recording site conditions, Bull. Seism. Soc. Amer. 66, 1343-1373.

Udwadia, F. E. and M. D. Trifunac (1974). Characterization of response spectra through the statistics of oscillator response, Bull. Seism. Soc. Amer. 64, 205-219.